Short title: Hydrogen cyanide regulation by S-cyanylation

Corresponding author:
Luis C. Romero
Instituto de Bioquímica Vegetal y Fotosíntesis, Consejo Superior de Investigaciones Científicas and Universidad de Sevilla
Avenida Américo Vespucio, 49,
41092 Seville, Spain
lromero@ibvf.csic.es

HCN regulates cellular processes through posttranslational modification of proteins by S-cyanylation

Irene García, Lucía Arenas-Alfonseca, Inmaculada Moreno, Cecilia Gotor and Luis C. Romero.

Instituto de Bioquímica Vegetal y Fotosíntesis, Consejo Superior de Investigaciones Científicas and Universidad de Sevilla, Avenida Américo Vespucio, 49, 41092 Sevilla, Spain

One-sentence summary

Hydrogen cyanide can act as a signaling molecule through posttranslational modification of protein cysteine residues, leading to S-cyanylation.

.

Author contributions:

I.G. and L.A-A. performed the experiments, I.G. and L.C.R. designed the experiments and analyzed the data; C.G. and L.C.R. supervised the experiments; I.M. provided technical assistance; L.C.R wrote the article with the contributions of all authors.

Funding:

This work was supported in part by the European Regional Development Fund through the Agencia Estatal de Investigación grant BIO2016-76633-P. L. A-A. was supported by the Ministerio de Economia y Competitividad through the program of Formación de Personal Investigador.

Correspondence: Luis C. Romero. E-mail: lromero@ibvf.csic.es

ABSTRACT

Hydrogen cyanide (HCN) is coproduced with ethylene in plant cells and is primarily enzymatically detoxified by the mitochondrial ß-CYANOALANINE SYNTHASE (CAS-C1). Permanent or transient depletion of CAS-C1 activity in Arabidopsis (*Arabidopsis thaliana*) results in physiological alterations in the plant that suggest that HCN acts as a gasotransmitter molecule. Label-free quantitative proteomic analysis of mitochondrially enriched samples isolated from the wild type and *cas-c1* mutant revealed significant changes in protein content, identifying 451 proteins that are absent or less abundant in *cas-c1* and 353 proteins that are only present or more abundant in *cas-c1*. Gene ontology classification of these proteins identified proteomic changes that explain the root hairless phenotype and the altered immune response observed in the *cas-c1* mutant. The mechanism of action of cyanide as a signaling molecule was addressed using two proteomic approaches aimed at identifying the S-cyanylation of cysteine as a posttranslational modification of proteins. Both the 2-imino-thiazolidine chemical method and the direct untargeted analysis of proteins using LC-MS/MS identified a set of 163 proteins susceptible to S-cyanylation that included SEDOHEPTULOSE 1,7-BISPHOSPHATASE (SBPase), the PEPTIDYL-PROLYL CIS-TRANS ISOMERASE 20-3 (CYP20-3), and ENOLASE 2 (ENO2). *In vitro* analysis of these enzymes showed that S-cyanylation of SBPase Cys^{74}, CYP20-3 Cys^{259}, and ENO2 Cys^{346} residues affected their enzymatic activity. GO classification and protein-protein interaction cluster analysis showed that S-cyanylation is involved in the regulation of primary metabolic pathways, such as glycolysis, and the Calvin and S-adenosylmethionine cycles.

INTRODUCTION

Hydrogen cyanide (HCN) is a gaseous acid produced in nature by a wide variety of microorganisms such as fungi, bacteria and algae (Knowles, 1976), as well as in cyanogenic plant food such as almonds (*Prunus dulcis*), millet sprouts (*Panicum miliaceum*), cassava roots (*Manihot esculenta*) or lima beans (*Phaseolus lunatus*), which are capable of accumulating significant amounts of cyanide, produced by the hydrolysis of cyanogenic glycosides (Hanschen et al., 2014; Baskar et al., 2016; Zidenga et al., 2017). Non-cyanogenic plant species also produce cyanide as a byproduct of some metabolic processes, such as during camalexin and ethylene biosynthesis (Peiser et al., 1984; Yip and Yang, 1988; Bottcher et al., 2009).

HCN can be partially dissolved in water and dissociates into H^+ and CN^- particularly in basic solutions. Because the cytosolic pH is close to 7, it is expected that cyanide would mostly present as hydrogen cyanide in this compartment, based on its pK of 9.3. The moderate lipid solubility and small size of the HCN molecule allow it to rapidly cross membranes and enter subcellular compartments. The anion cyanide is highly toxic because it reacts with Schiff base intermediates and keto compounds to produce cyanohydrins and nitrile derivatives, and because it chelates divalent and trivalent metal ions in metalloproteins. In mitochondria, it can bind to the heme iron of cytochrome c oxidase, inhibiting the functioning of the electron transport chain and acting as a potent inhibitor of respiration (Isom and Way, 1984). Cyanide is also a potent inhibitor of photosynthesis since it binds copper in plastocyanin, thereby inhibiting plastocyanin-dependent electron transport to Photosystem I (Berg and Krogmann, 1975) and dark CO_2 assimilation (Bishop and Spikes, 1955; Trebst et al., 1960). However, cyanide toxicity in chloroplasts occurs in the dark and is partially reversible by illumination in the presence of an electron acceptor (Bishop and Spikes, 1955; Cohen and McCarty, 1976).

Free cyanide, produced by metabolic pathways or by the degradation of cyanogenic glycosides, is detoxified by rhodanese or primarily assimilated into amino acids by the action of mitochondrial ß-cyanoalanine synthase (CAS-C1), a pyridoxal phosphate-dependent enzyme that uses cysteine to detoxify cyanide by converting the cyanide and cysteine into hydrogen sulfide (H_2S) and β-cyanoalanine (Ressler et al., 1969; Hatzfeld et al., 2000). The H_2S produced in the mitochondria inhibits cytochrome c oxidase as potently as cyanide and requires detoxification by the mitochondrial O-

acetylserine(thiol)lyase isoform, which catalyzes the incorporation of sulfide into O-acetylserine to produce cysteine, thus generating a cyclic pathway in the mitochondria (Alvarez et al., 2012; Nicholls et al., 2013).

Despite its toxicity, cyanide has been proposed to act as a regulator of several biological processes such as seed dormancy and germination (Taylorson and Hendricks, 1973; Bethke et al., 2006; Garcia et al., 2014), resistance to fungal and viral infection (Chivasa and Carr, 1998; Wong et al., 2002; Seo et al., 2011), susceptibility to the fungus *Botrytis cinerea,* and increased tolerance to the bacterium *Pseudomonas syringae* pv. *tomato DC3000,* as well as to the beet curly top virus (Lozano-Durán et al., 2012; Garcia et al., 2013). Arabidopsis (*Arabidopsis thaliana*) null mutants of the mitochondrial ß-cyanoalanine synthase, CAS-C1, accumulate cyanide to apparently nontoxic levels, as the plants are completely viable, but show a root hairless phenotype suggesting a signaling role in root development (Garcia et al., 2010; Garcia et al., 2014; Arenas-Alfonseca et al., 2018). The root hair defect is phenocopied by the addition of cyanide to the growth medium and reversed by the addition of the antidote hydroxocobalamin (Garcia et al., 2010; Thompson and Marrs, 2012). A fused CAS-C1-GFP protein under the control of the CAS-C1 promoter clearly localized in mitochondria, but showed a tip-preferred localization during root hair growth (Arenas-Alfonseca et al., 2018). Genetic crosses between the *cas-c1* mutant and the *scn1* or *rhd2* root hair mutants were performed, and the detailed phenotypic and molecular characterization of the double mutants demonstrated that the *scn1* mutation is epistatic to *cas-c1,* and *cas-c1* is epistatic to the *rhd2* mutation, indicating that CAS-C1 acts in the early steps of the root hair development process. In addition, CAS-C1 function is independent of ROS production and the direct inhibition of NADPH oxidase by cyanide (Arenas-Alfonseca et al., 2018).

Cyanide functions as a signaling molecule in the response to pathogens as indicated by the transient repression of the *CAS-C1* transcript and accumulation of cyanide when plants were infected with an avirulent *P. syringae* pv. *tomato DC3000 avrRpm1* strain (Garcia et al., 2013). Although transient cyanide accumulation in response to specific pathogens can induce a controlled accumulation of ROS for signaling purposes, a direct effect of cyanide as a signaling molecule cannot be excluded. The cyanide ion can attack cystine peptides or disulfides by nucleophilic displacement on a sulfur atom of the disulfide forming a thiocyanate derivative according to the reaction

136 $R\text{-}S\text{-}S\text{-}R + CN^- \leftrightarrows R\text{-}S^- + R\text{-}S\text{-}CN$

137 which may be considered a redox reaction (Gawron, 1966). This reaction may
138 occur at intra- and/or inter-chain disulfide linkages at pH 7.0; however, at alkaline pH,
139 the direction of the reaction would be towards the formation of the thiocyanate
140 derivative (Gawron, 1966; Wagner and Davis, 1966).

141 The reaction of cyanide with cystine-containing proteins results in the formation
142 of an S-cyanylated cysteine motif that cycles and is subsequently cleaved to release an
143 amino terminal-peptide at one end and a 2-imino-thiazolidine-4-carboxylyl COOH-
144 terminal peptide at the other (Catsimpoolas and Wood, 1966; Fasco et al., 2007). The
145 reaction of cyanide ions with disulfide bridges within polypeptides has been considered
146 to be similar to that of other small molecules, such as NO or H_2S, that react with Cys
147 residues to produce Cys modifications (Yamasaki et al., 2016; Aroca et al., 2017b;
148 Aroca et al., 2018).

149 In this study, we thoroughly examined the function of cyanide and the enzyme
150 ß-cyanoalanine synthase, which regulates the accumulation/detoxification of cyanide, in
151 the physiology of the cell through a proteomic approach. In addition, we analyzed the
152 molecular mechanism by which cyanide can act as a signaling molecule.

153

154

155 **RESULTS**

156

157 **Quantitative proteomic analysis of mitochondrial ß-cyanoalanine synthase CAS-**
158 **C1 null mutant**

159 The absence of ß-cyanoalanine synthase in the mitochondria results in a slight
160 increase in total cyanide in whole seedlings by 1.5-fold in the null *cas-c1* mutant and a
161 3-fold accumulation after treatment with the ethylene/cyanide precursor 1-
162 aminocyclopropane-1-carboxylic acid (ACC) (Garcia et al., 2010). To thoroughly
163 investigate the role of CAS-C1 in cellular physiology and decipher the functional
164 mechanism that explains the observed phenotype in the *cas-c1* mutant, we characterized
165 the protein composition and relative abundance of root extracts from wild type and *cas-*
166 *c1* mutants using proteomics SWATH-MS (Sequential Window Acquisition of all
167 THeoretical spectra-Mass Spectrometry) technology.

168 Protein samples were isolated from root hydroponic cultures using density-
169 gradient centrifugation aiming to obtain a better enrichment of mitochondrial proteins

(Table S1). Extracted proteins from three biological replicates of the wild type and three from the *cas-c1* mutant line were digested, and the peptide solutions analyzed by a shotgun data-dependent acquisition (DDA) approach to generate the spectral library. After integrating the six datasets, a total of 11,122 peptides (1% FDR and 96% confidence) and 1,734 unique proteins (1% FDR) were identified (Supplemental Dataset 1). To quantify them using SWATH acquisition, the same six biological samples were analyzed twice each (technical replicas) by a data-independent acquisition (DIA) method using the LC gradient and LC-MS equipment described to generate the spectral library, but instead using the SWATH acquisition method described in the Materials and Methods section. Therefore, for quantitation, six datasets from wild type and six from *cas-c1* were generated and used for the analysis. The fragment spectra were extracted for the twelve runs, and 2,035 ion transitions, 2,901 peptides, and 1,132 proteins were quantified. From the 1,132 quantified proteins (Supplemental Dataset 2), 551 had significantly different abundances in wild type and *cas-c1* (p value < 0.05) (Table S2). From these proteins, 97 were more abundant in the wild type exhibiting a fold change > 1.5, and 71 were more abundant in *cas-c1* with a fold change < 0.66. In addition to the differentially abundant proteins, we detected in the spectral library generated by the DDA approach that 354 proteins were only identified in the wild type samples and were below the detection limit in *cas-c1* (Table S3), and 282 were only identified in the *cas-c1* samples (Table S4).

The 451 proteins that were absent (354 proteins) or less abundant (97 proteins) in *cas-c1* were analyzed based on their assigned functions and classified into 28 functional groups (Table S5) using the MapMan nomenclature (Thimm et al., 2004; Klie and Nikoloski, 2012). The most numerous sets corresponded to the general protein group (bin 29), which included 17.1% of the total identified proteins with 77 elements involved in protein degradation (25 elements, primarily of the ubiquitin-proteasome system), protein synthesis (20 elements), subcellular targeting (11 elements) and posttranslational modification (10 elements). Many of the proteins identified are related to pathogen response and biotic stress (Supplemental Fig. S1A), and GO classification highlighted an important group containing proteins involved in signaling (13.3%) with 60 elements. Interestingly, 26 proteins of the receptor kinase family functioning in pathogen response are present in this group and include six leucine-rich repeat protein kinases, six domain of unknown function 26 (DUF26) receptor proteins and two lectin kinases (Supplemental Fig. S1B and Table S5). Previous proteomic analyses in potato

(*Solanum tuberosum*) and Arabidopsis have also shown the presence of a significant number of protein kinases in plant mitochondria related to communication and signaling (Salvato et al., 2014; Rao et al., 2017). However, some DUF26 receptors are cytosolic or plasma membrane proteins and were detected in this proteomic analysis because although the protein preparation was enriched in mitochondria, it also contained other membranes and organelles.

The 353 analyzed proteins that were only present (282 proteins) or more abundant (71 proteins) in *cas-c1* compared to the wild type were classified into 28 functional groups using MapMan (Table S6). Once again, the most abundant set classified into the protein group with 59 elements involved in protein synthesis (22 elements), protein degradation (14 elements), subcellular targeting (9 elements) and posttranslational modification (9 elements). An overrepresentation test of the GO terms using PANTHER DB´s tool (Mi et al., 2017) to examine the abundant proteins showed a 9.52-fold enrichment of proteins involved in the regulation of carbohydrate metabolism, including four nuclear transcription factors NF-YC1, NF-YC3, NF-YC4 and NF-YC9; 9.33-fold enrichment in cellular amino acid catabolism and 7.35-fold enrichment in ras-related proteins involved in phagocytosis and membrane trafficking (Table S7).

Finally, to determine the functional relevance of the *CAS-C1* mutation in the physiology and development of the plant, we used the STRING database v10.5 (Szklarczyk et al., 2015) to analyze the protein-protein interaction network of the 353 proteins with increased abundance in *cas-c1* compared to the wild type to determine functional association of those proteins. Using the highest confidence (interaction score 0.900), a total of 295 protein-protein interactions were observed, and they were significantly enriched (p-value < 0.000655) based on the given protein nodes. At least four protein clusters that are biologically connected were clearly distinguished after analysis (Fig. 1). The first cluster contains a subgroup with a complex of 17 ribonucleoproteins (yellow nodes) linked to a second cluster of 8 proteins of the spliceosome pathway (red nodes), which is also connected through the E3 ubiquitin ligase MAC3B component of the MOS4-associated complex to a subgroup containing several cyclin-dependent kinases (CDKC1, CDKC2, CDKD1, CDKD3) and ubiquitin-specific protease 12 and 13 (UBP12, UBP13). A third important cluster (blue nodes) centered in ELI3-2 (ELICITOR ACTIVATED GENE 3-2) and CYP84A1 (ferulic-acid 5-hydrolase), both involved in lignin biosynthesis, comprises 8 peroxidase proteins

(PER7, PER16, PER23, PER27, PER32, PER44, PER45 and PER49) and IRX4 (cinnamoyl CoA-reductase, involved in the latter stages of lignin biosynthesis). The fourth cluster (green nodes), centered on RAB GTPas-1A, comprises several subgroups with proteins involved in the endomembrane system, regulators of membrane traffic from the Golgi apparatus towards the endoplasmic reticulum, and includes RAB GTPase-1b, 1c and 8C and 5 coatomer subunit proteins. This cluster also contains a subgroup formed by 4 nuclear transcription factors, NF-YC1, NF-YC3, NF-YC4 and NF-YC9 that regulate gene expression by modulating histone acetylation and methylation.

Identification of S-cyanylation by the chemical 2-imino-thiazolidine method

The cyanide molecule possesses physico-chemical characteristics similar to well-established signaling molecules such as NO, CO, or H_2S (Gotor et al., 2017). In addition to its affinity for metalloproteins, cyanide does not react with free thiol groups but can react with cystine-containing proteins at cellular neutral and mild alkaline pH and, by analogy to NO or H_2S, modify protein residues, which subsequently alters protein function. To explore the function of cyanide as a signaling molecule through protein posttranslational modifications (PTMs), we studied the presence of proteins with S-cyanylated-cysteine residues in cytosolic leaf and root extracts.

It is well described that S-cyanylated proteins can be cleaved into two parts, the amino acid backbone from the N-terminus to the cyanilated cysteine residue and the cycled 2-imino-thiazolidine-4-carboxylyl COOH-terminal peptide (Fig. 2A) (Catsimpoolas and Wood, 1966; Fasco et al., 2007), a process that is favored at alkaline conditions. Considering the above chemical properties of S-cyanylated cysteines, we studied *in vitro* the endogenous presence of this modification in leaf protein extracts from Arabidopsis wild type and *cas-c1* mutant lines. Depletion of CAS-C1 activity results in the accumulation of cyanide in 2-week-old seedlings, and this accumulation can be increased by treatment with ACC, the precursor of ethylene and cyanide, via ACC oxidases (Garcia et al., 2010). Therefore, the presence of endogenous S-cyanylated proteins was analyzed in 2-week-old wild-type and *cas-c1* leaves treated with 100 µM ACC for 24 h by comparing the mobility shift or spot volume of the proteins after cleavage with 1 M NH_4OH (Fig. 2B) by the 2-imino-thiazolidine chemical method. The protein samples from 2-week-old leaves were treated with NH_4OH for 1 h or 0.01 M NaOH as a control and separated by two-dimensional (2D) isoelectric

focusing (IEF)-SDS polyacrylamide gel electrophoresis (PAGE). Three replicate samples were subjected to 2D IEF-SDS PAGE, stained with Coomassie-blue, scanned by a densitometer and the protein spots quantified using image analysis software (Fig. 2B). More than 400 protein dots were resolved in the 2D-gel, and 42 proteins in the three replicates from the wild-type leaves showed different electrophoretic mobility or spot volume after alkaline digestion with NH_4OH compared to the control samples at mild alkaline treatment, and the number increased to 72 in the *cas-c1* leaf samples, resulting in 88 different proteins (Table S8). Twenty-six proteins were present in both genetic backgrounds suggesting that S-cyanylation may occur independently of the absence or presence of ß-cyanoalanine synthase activity after the induction of ethylene synthesis. Interestingly, one of these proteins was 1-AMINOCYCLOPROPANE-1-CARBOXYLATE OXIDASE 2, which is responsible for the co-biosynthesis of ethylene and cyanide from ACC. Two of the proteins with different electrophoretic mobility were the chloroplastic sedoheptulose-1,7-bisphosphatase (SBPase) and the peptidyl-prolyl cis-trans isomerase (CYP20-3) (Fig. 2B).

Gene Ontology term enrichment analysis for biological processes using the PANTHER DB´s tool (Mi et al., 2017) showed an overrepresentation among S-cyanylated proteins of those involved in glycolysis, with a 65-fold enrichment, and in the Calvin cycle. The GO analysis of S-cyanylated proteins by cellular components in the *cas-c1* lines showed an enrichment in proteins of the phosphopyruvate hydratase complex, including ENOLASE 1 and 2 (ENO1 and ENO2) with >100-fold enrichment (Table S9), which are known to be associated with other glycolytic enzymes on the surface of Arabidopsis mitochondria (Giege et al., 2003).

Identification of S-cyanylation by mass spectrometry

To further evaluate the presence of this modification in the Arabidopsis proteome, we also analyzed the presence of S-cyanylated cysteines in root tissues from wild-type plants using mass spectrometry to complement the chemical 2-imino-thiazolidine method. For this purpose, we compared root tissues untreated or treated with ACC as a generator of cyanide and utilized high resolution MS to determine the presence of peptides containing cysteine residues with cyanide modification, which would result in a 25.0095 Da mass increase in the fragmentation spectrum. Although this modification has been poorly studied, there are some reports that have detected S-cyanocysteine modifications using mass spectrometry (Bishop and Spikes, 1955;

306 Fricker, 2015). For protein identification, we used three biological replicate samples of
307 total protein extracts from root tissues untreated or 100 µM ACC-treated for 24 h, and
308 identified a total of 2,442 proteins present in the three replicates of treated roots and
309 2,325 in the three replicates of the untreated samples (Supplemental dataset 3). From
310 these, 30 proteins in the untreated roots and 50 proteins in the treated roots, representing
311 64 different proteins, were found to contain an S-cyanylation-Cys modification. A total
312 of 67 peptides were identified from the 64 different proteins, which constitute 1.4% of
313 the proteins identified in roots (Table 1). Moreover, in the SWATH proteomic analysis
314 described earlier, we identified 11 additional peptides that were modified by S-
315 cyanylation, which were added to the list of proteins identified using LC-MS/MS (Table
316 S10).
317 All the proteomic approaches described in this study have allowed us to identify
318 a total of 163 different proteins susceptible to S-cyanylation: 88 unique proteins using
319 the 2-imino-thiazolidine chemical method and 75 proteins using the LC-MS/MS method
320 (Table S10). The S-cyanylated proteins identified were analyzed based on their assigned
321 functions and classified into 28 functional groups using the MapMan nomenclature. The
322 most abundant set corresponded to the general protein group, which included 13% of
323 the total identified proteins with 22 elements, and the photosynthesis bin with 19
324 elements, which included the small and the large subunit of ribulose bisphosphate
325 carboxylase (RUBISCO) and several other enzymes of the Calvin cycle and glycolysis
326 including ENO1 and ENO2.
327 To examine the function of S-cyanylation in metabolism and regulatory
328 processes in more detail, the 163 S-cyanylated proteins were analyzed using the
329 STRING database v10.5. Using the highest confidence (interaction score 0.900), a total
330 of 193 protein-protein interactions were observed, and they were significantly enriched
331 (p-value < 1.0 e^{-16}) based on the given protein nodes, suggesting that they are
332 biologically connected. *k*-means clustering analysis of the protein-protein interaction
333 network identified four clusters of proteins with important biological functions (Fig. 3).
334 The cluster containing the most proteins (red nodes) includes proteins involved in
335 several metabolic processes such as protein folding, including CHAPERONIN-
336 60ALPHA (CPN60A), CHAPERONIN-60BETA2, chloroplast and mitochondrial heat
337 shock proteins HSP70-1 and HSP70-2, ROTAMASE FKBP-1 (ROF1) and other HSPs.;
338 the TCA cycle, including ACONITASE 1 (ACO1) and 2 (AT4G26970); isocitrate
339 dehydrogenases (ICDH and cICDH), and response to stress including the beta-

glucosidases BGLU21, BGLU22, BGLU23/PYK10. Members of this group (RBCL and RBCS) are connected to a second cluster (yellow nodes), which includes proteins involved in carbon fixation and glycolysis/gluconeogenesis, such as ENO1 and ENO2/LOS2, GLYCERALDEHYDE-3-PHOSHPHATE DEHYDROGENASE A (GAPA), and several phosphoglycerate kinases and aldolases (Fig. 3 and Fig. S2). A third cluster (blue nodes) comprises enzymes of the S-adenosyl methionine cycle centered in METHIONINE OVER-ACCUMULATOR 3 (MTO3), essential in DNA and histone methylation, and includes DNA METHYLTRANSFERASE 2 (DMT2), METHIONINE SYNTHASE 1 and 2 (ATMS1, ATMS2) and S-ADENOSYL-L-HOMOCYSTEIN HYDROLASE 1 (SAHH1). The last cluster (green nodes) contains several ribosomal proteins involved in protein synthesis.

Identification of S-cyanylated Cys residues of representative proteins

To demonstrate that Cys residues are indeed modified by S-cyanylation, and to identify the modified residues of representative proteins identified by the chemical 2-imino-thiazolidine method, we conducted liquid chromatography-tandem mass spectrometry (LC-MS/MS) analyses of SBPase and CYP20-3. Recombinant proteins were purified from bacterial extracts, trypsin-digested and the digested peptides were analyzed using LC-MS/MS to identify a 25.0095 Da mass increase in the fragmentation spectrum. As illustrated in Figure 4 (Fig. 4) (Table S11), the SBPase enzyme was identified with a sequence coverage of 67% and among the peptides identified, the peptide SNGASTVTKCEIGQSLEEFLAQATPDK, containing Cys^{74}, showed S-cyanyl modification. The Cys^{116} and Cys^{121} residues that form a disulfide bridge and can be redox regulated by thioredoxin f were not detected as S-cyanylated. In the same manner, as SBPase, the CYP20-3 protein was analyzed by LC-MS/MS. The protein was identified with a sequence coverage of 61% and Cys^{206} within the peptide HTGPGILSMANAGPNTNGSQFFICTVK was identified as S-cyanylated (Fig. 5) (Table S12). The activity of CYP20-3 is controlled by thioredoxin-mediated redox regulation of the two disulfide bridges between Cys^{131}-Cys^{248} and Cys^{206}-Cys^{253} and the enzyme is fully enzymatically inactive in the oxidized state (Motohashi et al., 2003). The redox state of CYP20-3 was determined by analysis of the redox-dependent electrophoretic mobility of the protein under oxidizing and reducing conditions. Proteins with reduced cysteine residues can be alkylated and therefore run more slowly during electrophoresis than oxidized proteins that cannot be alkylated. Treatment with

H_2O_2 oxidized the Cys residues of CYP20-3 inducing formation of disulfide bridges, which changed its mobility such that it migrated more quickly than the reduced and iodoacetamide-alkylated protein (Fig. 6A). When the oxidized protein was subsequently treated with cyanide, its mobility was reduced due to the rupture of the disulfide bridge by S-cyanylation. However, rupture of the disulfide bridges by cyanide treatment did not reactivate the enzymatic activity, which could only be partially recovered after reduction with DTT (Fig. 6B).

The effect of S-cyanylation on ENO2, identified in the two proteomic approaches, was also analyzed. Enolase is a multifunctional enzyme that has catalytic activity in glycolysis, converting 2-phosphoglycerate into phosphoenolpyruvate, and also acts as a regulator of gene transcription (Lee et al., 2002). Arabidopsis ENO2 contains five Cys residues in its sequence, but we found that only Cys^{346} within the peptide SCNALLLK was modified by S-cyanylation (Fig. 7 and Table S13). We measured the effect of oxidation using H_2O_2 treatment and observed a significant increase in enzymatic activity due to Cys oxidation and the resulting formation of disulfide bridges (Fig. 8). This result is consistent with data previously observed for some other plant enolases from Arabidopsis, tomato (*Solanum lycopersicum*), and the ice plant *Mesembryanthemum crystallinum*, which may form a disulfide bridge between Cys^{313} and Cys^{338} (according to the maize *(Zea mays*) sequence) at the C-terminal active site of the enzyme. Its activity can be slightly inhibited by DTT and can be activated approximately 2-fold by the oxidant diamine (Anderson et al., 1998). Further treatment with cyanide after the H_2O_2 oxidation increased the enzymatic activity of the Arabidopsis ENO2 by >50% (Fig. 8). Enolase has been identified to be a target of thioredoxin in several proteomic studies, but *in vivo* studies and the regulatory Cys residues have not been reported.

DISCUSSION

Changes in the *cas-c1* proteome explains the root hair defect and altered response to pathogens

Hydrogen cyanide is produced in plants by several metabolic processes, but in non-cyanogenic plants, ethylene biosynthesis is thought to be the primary source (Yip and Yang, 1988). Therefore, during many developmental or environmental stress processes where ethylene is produced, the amount of co-synthesized HCN can be

substantial. HCN can be removed or detoxified either by enzymatic activities (rhodanese and ß-cyanoalanine synthase) or, due its own chemical reactivity, reaction with organic molecules susceptible to nucleophilic attack like disulfide bridges, such as cystine, oxidized glutathione and organic persulfides, producing the corresponding thiocyanate, and reaction with aldehydes and ketones to produce cyanohydrins (Gawron, 1966; Park et al., 2015). Thus, plants have evolved mechanisms to control cyanide levels and avoid its toxic effects. Although the high reactivity of HCN makes it very toxic, it is interesting to note that transcript levels of *CAS-C1* are transiently repressed, with the corresponding accumulation of cyanide, after infection with an avirulent *Pst* DC3000 *avrRpm1* strain, indicating that there are defined programs in the cell to allow the accumulation of cyanide probably for signaling purposes (Garcia et al., 2013; Garcia et al., 2014; Romero et al., 2014). In fact, cyanide has chemical characteristics very similar to other gasotransmitters such as nitric oxide (NO), carbon monoxide (CO) and hydrogen sulfide (H_2S) and meets all the criteria to be classified as one (Tinajero-Trejo et al., 2013; Wang, 2014).

Together with the quantified changes in root hair growth and pathogen response induced by the *CAS-C1* mutation, molecular phenotyping by proteomic analysis of *cas-c1* can identify pathways that contribute to the observed phenotypic changes (Fig. 1) (Garcia et al., 2010; Garcia et al., 2013; Arenas-Alfonseca et al., 2018). The decrease in the ability to enzymatically detoxify cyanide in the mitochondria results in the accumulation of proteins involved in the initial elongation phase of root hair growth, such as GTPases and cell wall modification enzymes (Grierson et al., 2014). One of these groups includes RAB GTPase-1A, other RAB GTPases, and several coatomer subunit proteins, which function in the endomembrane system to regulate membrane traffic from the Golgi apparatus toward the endoplasmic reticulum. Since the polarized expansion of root hairs depends on the formation and delivery of cell wall components to the growing tips, changes in the RAB GTPase composition and activity may alter the formation and delivery of secretory vesicles from the trans-Golgi network. In addition to the membrane trafficking protein clusters, the *CAS-C1* mutation regulates and induces the accumulation of groups of proteins involved in lignin biosynthesis for cell wall formation, which suggests an increased accumulation of lignin that may inhibit or hinder the cell wall relaxation for tip growth. Previous transcriptional data from root tissues (Garcia et al., 2010) revealed the repression of several well-known genes related to root hair formation, such as *MRH5/SHV3*, *MRH6* and *XTR9*, encoding

arabinogalactan proteins, xyloglucan:xyloglucosyl transferases, endotransglycosylase, pectinesterases and pectate lyase proteins that have been correlated with the organization of cortical microtubules that influence root epidermal expansion and morphogenesis (Nguema-Ona et al., 2007). Since the site of bulge formation requires that the trichoblast locally loosens its cell wall, this process must be interfered with in *cas-c1*. Transcriptomic and proteomic data are thus consistent with the interpretation that cyanide regulates root hair formation by altering cell wall formation and relaxation at the elongation zone of the hair to prevent its expansion and explains the root hairless phenotype of the *cas-c1* mutant.

The second process identified in which cyanide plays a physiological role is related to the response to pathogens (Chivasa and Carr, 1998; Seo et al., 2011; Garcia et al., 2013). From the GO classification of the proteins that are less abundant or absent in *cas-c1*, we can highlight those involved in signaling, which include 26 proteins of the receptor-like kinase (RLK) family that are conserved signaling components that regulate developmental programs and biotic stresses (Supplemental Fig. S1 and Table S5) (Tang et al., 2017). Among these, there are six cysteine-rich RLK DOF26 proteins with a DOF domain, which has four conserved cysteines that may form disulfide bridges as potential targets for thiol redox regulation (Chen, 2001). In addition to the RLKs, many proteins involved in biotic stress are unbalanced in abundance in *cas-c1*, such as the basic-leucine zipper (bZIP) transcription factors POSF21 and WRKY52/RRS1, which confer resistance to *Ralstonia solanacearum* (Williams et al., 2014), and may also explain the increased susceptibility to necrotrophic fungi. The *CAS-C1* mutation also induces the accumulation of a cluster of proteins that include the MAC3B protein, a component of the MOS4-associated complex, which regulates the response to pathogens by regulating *SUPPRESSOR OF NPR1-1 CONSTITUTIVE 1 (SNC1)* (Monaghan et al., 2009), and the deubiquitinating enzymes UBP12 and UBP13, which regulate the transcription factor MYC2 (Jeong et al., 2017). Therefore, the accumulation of cyanide induces significant transcriptional and proteomic changes in the cell consistent with the alterations in development and pathogen response observed by ß-cyanoalanine synthase depletion (Garcia et al., 2013).

Cyanide posttranslationally modifies cysteine residues on proteins

Although cyanide has been proposed to act as a signaling molecule, the mechanism behind this role remains unknown. Based on its chemical reactivity, cyanide

476 can act by forming adducts with the metal centers in proteins that contain iron or cobalt.
477 The cyano-iron complex in the heme prosthetic groups of metalloproteins inhibits the
478 activity of enzymes such as cytochrome c oxidase. A second mechanism involves the
479 posttranslational modification of protein cysteine residues leading to the S-cyanylation
480 of the protein. This process was thought not to take place under physiological
481 conditions in any organism, however S-cyanylated-Cys residues in human plasma
482 proteins, such as immunoglobulin G and serum albumin, are detected after cyanide
483 poisoning or in smoking persons and are used as biomarkers of potential cyanide
484 exposure (Fasco et al., 2007; Grigoryan et al., 2016). We have here identified S-
485 cyanylated-Cys residues in the proteins of leaf and root samples, in addition to
486 characterizing the molecular changes produced by genetic ß-cyanoalanine synthase
487 depletion and concomitant cyanide accumulation. Using two different physicochemical
488 approaches, the 2-imino-thiazolidine chemical method and direct untargeted analysis of
489 proteins using LC-MS/MS, we found that this modification occurs during physiological
490 growth conditions in leaf and root tissues, but can be increased by stimulating the
491 biosynthesis of ethylene and the concomitant cyanide production by treatment with the
492 ACC precursor. Although the number of S-cyanylated proteins detected is not high
493 (Table 1), we are probably underestimating the true number since we are only
494 identifying abundant proteins. Many PTMs such as carbonylation, nitrosylation,
495 persulfuration or nitration are identified using chemical labelling methods or by specific
496 antibodies, but so far we do not have available a method to enrich selectively for S-
497 cyanylated-Cys proteins that will allow us to purify and identify them (Alvarez et al.,
498 2011; Moller et al., 2011; Zhang et al., 2014; Aroca et al., 2017a).
499
500 **Role of S-cyanylation in cellular processes**
501 Both methods used to identify the S-cyanylated Cys residues detected the ENO2
502 protein encoded by the *LOS2/ENO2* locus, which functions in glycolysis for the
503 dehydration of 2-phosphoglycerate to produce phosphoenolpyruvate or acts as a
504 repressor of *cMyc* transcription by alternative translation of the locus to produce MBP-1
505 (Lee et al., 2002; Eremina et al., 2015). GO classification, enrichment and clustering
506 analysis of the 163 proteins that were identified to be susceptible to S-cyanylation
507 highlighted the role of these proteins in primary carbon fixation, glycolysis, the TCA
508 cycle and in general, carbon metabolism, but also in chaperone-assisted protein folding
509 and SAM-cycle/DNA methylation (Fig. 9). The *in vitro* analyses performed with some

of the identified S-cyanylated proteins showed that S-cyanylation of CYP20-3 results in the partial inhibition of its activity but results in the activation of ENO2. Since cyanide action against cysteine residue only takes place over oxidized cysteines in the form of disulfide bridges, the effect of S-cyanylation depends on the redox state of the target protein. CYP20-3 can form two disulfide bridges, which are required for its isomerase activity and are subject to regulation by thioredoxin (Motohashi et al., 2003), but S-cyanylation of Cys^{206} in its oxidized state results in the irreversible inactivation of its activity. Most of the enzymes of central carbon metabolism, photosynthetic carbon fixation, glycolysis and the TCA cycle are known to be light/dark regulated; therefore, they are inhibited in the dark by the oxidation of active site cysteines, but reactivated in the light by the action of ferredoxin/thioredoxin systems (Buchanan and Balmer, 2005; Geigenberger et al., 2005). Therefore, cyanide modification of these enzymes in their oxidized state must result in the irreversible inactivation of their activity as shown with CYP20-3. In this case, we can hypothesize that S-cyanylation acts as a switch to definitively stop the light/dark regulation of this activity under some specific conditions.

ENO2 activity, the ninth step of glycolysis, is higher during oxidative conditions and during KCN treatment, which indicates that S-cyanylation switches on the enzyme activity (Fig. 8 and (Anderson et al., 1998)). Thus, S-cyanylation can accelerate the degradation of sugar for ATP production to compensate for the inhibition of the cytochrome oxidase pathway. The *cas-c1* mutant shows higher transcript levels of the alternative oxidase *AOX1a* and higher respiration rates, but the levels of ATP are unaltered (Garcia et al., 2010; Arenas-Alfonseca et al., 2018). Thus, transient cyanide accumulation associated with developmental or environmental stress can potentially generate metabolic perturbations through the inhibition of enzymes of central carbon metabolism and the induction of the AOX gene that controls the production of signaling molecules such as ROS.

A second cyanide signaling mechanism might be the direct effect of S-cyanylation on protein localization. Many of the enzymes identified as susceptible to S-cyanylation, such as the glycolytic enzymes, including ENO2 and GAPDH, and proteins of the SAM-cycle, are moonlighting proteins involved either in metabolic pathways and gene transcription, but they lack nuclear localization sequences (Lee et al., 2002; Zaffagnini et al., 2013; Boukouris et al., 2016). Several of the enzymes of the glycolytic pathway are redox regulated and are more active in their reduced form, such as glyceraldehyde 3-phosphate dehydrogenase (Holtgrefe et al., 2008). However,

posttranslational modification of the cytosolic GAPDH GapC isoform by S-persulfidation of Cys^{160} slightly regulates its activity, but is critical to determine the cytosolic/nuclear partitioning of the enzyme (Aroca et al., 2015; Aroca et al., 2017b). In addition to its enolase activity, the *LOS2/ENO2* locus can be alternatively translated from a second AUG translation initiation codon at position +93 to form the protein *C-MYC BINDING PROTEIN 1* (MBP-1), which was found to bind *c-myc*-like elements in the promoter of the *STZ/ZAT10* gene acting as a transcriptional repressor (Lee et al., 2002). Both ENO2 and MBP-1 contain the Cys^{346} identified as being susceptible to S-cyanylation (Fig. 7). Although we have not tested the effect of S-cyanylation in the nuclear localization of ENO2 or the MBP-1 protein, previous transcriptomic analyses show the repression of *STZ/ZAT10* in the root tissue of *cas-c1,* suggesting the predominant nuclear localization of MBP-1 (Garcia et al., 2010).

In addition to the glycolytic enzymes, we also detected a large number of S-cyanylated proteins involved in the S-adenosyl-L-methionine (SAM) cycle and DNA and histone methylation such as methionine synthase MS1 and MS2, S-adenosyl-L-homocysteine hydrolase SAHH1/HOG1, SAHH2, and DNA METHYLTRANSFERASE 2 (DMT2). Methylation occurs in the nucleus through the metabolite S-adenosylmethionine, which functions as the primary methyl group donor, and the action of methytransferases that transfer the methyl group of SAM producing S-adenosyl-L-homocysteine (SAH), which is a potent inhibitor of methyltransferase activity (Sauter et al., 2013). SAHH1/HOG is localized either in the cytoplasm or nucleus, but it lacks any nuclear localization signal (Lee et al., 2012). Null T-DNA insertional mutants in *SAHH1*gene, *hog1* mutant, shows embryo-lethal phenotypes (Rocha et al., 2005). However, an *sahh1* mutant that produces the normal SAHH1 protein, but in reduced amounts, maintains its fertility level but shows a deficiency in root hair development (Wu et al., 2009). Since the S-cyanylation of SAHH1 does not result in the severe embryo-lethality of *cas-c1*, the Cys modification may be affecting the nuclear localization of the protein rather than inhibiting the SAHH1 activity. Based on all previous data, we suggest that the effect of S-cyanylation on protein localization is plausible and deserves further investigation.

CONCLUSION

In this study, we demonstrate that the accumulation of cyanide by the repression of the ß-cyanoalanine synthase activity may induce a nonenzymatic PTM into the Cys

motif. Although many nonenzymatic PTMs have been proposed to be indicators of different cellular stresses and used as biomarkers of aging, such as the oxidation of several amino acids, carbonylation or carbamylation, these modifications can also occur in nonstressed and healthy cells and can regulate and influence nonpathogenic cellular processes (Moller et al., 2011; Harmel and Fiedler, 2018). Unlike other nonenzymatic PTMs such as nitrosylation, disulfide formation and acylation, S-cyanylation seems to be a nonreversible modification since reductants cannot reverse its effect in the analyzed proteins. The fact that S-cyanylaton occurs on oxidized cysteines in the form of disulfide bridges can cause a change in the properties and function of the proteins. However, a much more extensive study on the effect of this PTM will be necessary to fully understand the functionality of this modification.

MATERIALS AND METHODS

Plant material and growth conditions

Arabidopsis (*Arabidopsis thaliana*) wild type ecotype Col-0 and the *cas-c1* T-DNA insertion mutant (*cas-c1*; SALK_103855) (Garcia et al., 2010) were grown in soil in a photoperiod of 16 h of white light (120 μmol m^{-2} s^{-1}) at 20 ºC and 8 h of dark at 18 ºC or in hydroponic culture in a photoperiod of 8 h of white light (120 μmol m^{-2} s^{-1}) at 20 ºC and 16 h of dark at 18 ºC (Bermudez et al., 2010). For the hydroponic cultures, seeds were surface-sterilized, incubated for 4 days at 4º C and germinated for one week in rockwool. Seedlings were introduced in the wells of hydroponic boxes containing 5 L of nutrient solution. The composition of the nutrient solution was as follows: 1 mM KH_2PO_4, 1 mM $MgSO_4 \cdot 7H_2O$, 15 μM $MnSO_4 \cdot H_2O$, 1 μM $CuSO_4 \cdot 5\ H_2O$, 1 μM $ZnSO_4 \cdot 7\ H_2O$, 30 μM H_3BO_3, 28 nM $(NH_4)_6Mo_7O_{24} \cdot 4\ H_2O$, 100 nM $CoSO_4 \cdot 7\ H_2O$, 10 mM $Ca(NO_3)_2 \cdot 4\ H_2O$ and 90 mM sequestrene 138 Fe G100 (Syngenta, Spain). All nutrient solutions were changed twice per month.

Mitochondrial protein extraction

Mitochondria-enriched samples were isolated from Arabidopsis roots using differential and density-gradient centrifugation as described (Struglics et al., 1993) but with modifications. A total of 30 g of Arabidopsis hydroponic root tissue was ground using a mortar and pestle with liquid nitrogen and resuspended into an extraction buffer

containing 15 mM MOPS (pH 7.4), 1.5 mM EDTA, 0.25 M sucrose, 0.4% (w/v) BSA and 0.6% (w/v) PVP-40, using 3 ml of buffer g^{-1} fresh weight, and the homogenates were filtered through two layers of Miracloth (Calbiochem). The filtered homogenate was centrifuged at 2200 g for 5 min and the supernatant transferred to a new tube, centrifuged again sequentially at 3200 g and 4500 g each time for 5 min until a non-green supernatant was obtained. This final supernatant was centrifuged at 18000 g for 30 min. The pellet was resuspended in 1 ml of gradient buffer (20 mM MOPS, pH 7.2, 0.6 M sucrose). The separation of the cellular organelles was obtained using a self-generated 45 and 27% Percoll gradient. The gradient was centrifuged at 20000 g for 20 min in an ultracentrifuge using an SW28.1 Ti rotor (Beckman) at 4°C. The mitochondrial band was taken out, diluted 10 times with the wash buffer (0.3 M sucrose, 1 mM EDTA, 10 mM MOPS at pH 7.2), and centrifuged at 20000 g for 15 min four times to wash the organelles free from Percoll. The last pellet was resuspended in 300 µL of lysis buffer (50 mM potassium phosphate buffer, pH 7.0, and 0.1% (v/v) Triton X-100) and the mitochondrial samples disrupted using repeating freeze-thaw cycles and ultrasonic lysis for 1.5 min. The samples were centrifuged at 20000 g for 15 min. Proteins from the supernatant were precipitated with 10% (v/v) trichloroacetic acid and ice-cold acetone and resuspended in 20 mM Tris-HCl, pH 8.0.

Identification of protein S-cyanylation using the 2-imino-thiazolidine chemical method

Arabidopsis cytosol-enriched leaf protein extract was isolated to perform 2D electrophoresis. For this, 200 mg of frozen leaf tissue was ground in liquid nitrogen using a mortar and pestle. The resulting powder was homogenized in 2 mL of water and ultracentrifuged at 176000 g for 1 h at 4 °C. The protein concentration in the supernatant was then quantified and used for the ammonium hydroxide treatment. Four hundred micrograms of protein were incubated with 1 M of ammonium hydroxide or 0.01 M of sodium hydroxide for 1 h at 20ºC. Proteins were then dried in a speed vacuum, resuspended in 300 µL of 1 mM Tris - 10 mM EDTA, pH 7.5, and precipitated with 10% TCA (v/v) overnight at 4ºC, centrifuged at 20000 g for 15 min at 4ºC, and the pellet washed twice with 100% acetone. After the final centrifugation step, the protein pellet was air-dried and resolubilized in 8 M urea, 2% (w/v) CHAPS, 50 mM dithiothreitol, 0.2% (v/v) ampholytes (Bio-Lyte 3-10 buffer, Bio-Rad), and a trace of bromophenol blue.

The proteins were applied to a linear immobilized pH gradient strip, pH 4 to 7 during rehydration. Isoelectric focusing was performed at 22°C in the Protean IEF Cell (Bio-Rad) in three steps: (1) 250 V for 15 min, (2) 10,000 V for 1 h, and (3) 10,000 V up to 40,000 V. The intensity was fixed at 50 μA per immobilized pH gradient strip to avoid overheating the system. For the second dimension analysis, the equilibrated gel strips were placed on top of vertical polyacrylamide gels (12% w/v acrylamide and SDS) (Laemmli, 1970). Electrophoresis was conducted at 240 V and 35 mA per gel for 5 h using the Protean II xi Cell (Bio-Rad). Protein spots were visualized after Coomassie brilliant blue staining.

The 2D images were analyzed using laser densitometry scanning with a GS-800 calibrated densitometer (Bio-Rad), and three high-quality gels from independent protein extracts and conditions were analyzed using the PDQuest software version 7.0 (Bio-Rad). Protein spots of interest were excised, trypsin digested and identified using MALDI-mass spectrometry analysis at the Proteomic Facility of the Institute of Plant Biochemistry and Photosynthesis as previously described (Bermudez et al., 2012)

Identification of S-cyanylated proteins using LC-MS/MS analysis

To identify S-cyanylated proteins, tryptic digestion was performed in solution of root extracts, and peptide analysis was carried out using a nano liquid chromatography system coupled to a high-speed mass spectrometer at the Proteomics Facility of the Centro Nacional de Biotecnología, Spain. An aliquot of 40 μg of protein from each treatment group was digested with sequencing-grade modified trypsin (Sigma-Aldrich) at 37 ºC overnight on a shaker. Three biological replicates for both conditions (wild type and *cas-c1*) were analyzed using the same setup and the parameters previously described (Aroca et al., 2017a).

The mass spectrometry data have been deposited in the ProteomeXchange Consortium via the PRIDE (Vizcaino et al., 2016) partner repository with the dataset identifier PXD009812.

Protein function analysis and classification was performed using MapMan (Thimm et al., 2004; Klie and Nikoloski, 2012) and clustering analysis by using the STRING database (Szklarczyk et al., 2015). The protein-protein association network was assessed in STRING using interaction evidences coming from experimental data on protein-protein interactions, interaction prediction from co-expression analysis, and

known pathways and protein complexes from curated databases and co-occurrence in publications (Szklarczyk et al., 2015; Szklarczyk et al., 2017)

Protein relative quantitation by SWATH-MS acquisition and analysis

Protein samples from mitochondrial extracts for SWATH-MS measurements were alkylated and trypsin-digested as described (Vowinckel et al., 2013; Ortea et al., 2018), and performed at the Proteomic Facility of the Insituto Maimónides de Investigación Biomédica de Córdoba, Spain.

A data-dependent acquisition (DDA) approach using nano-LC-MS/MS was first performed to generate the SWATH-MS spectral library as described (Ortea et al., 2018).

The peptide and protein identifications were performed using Protein Pilot software (version 5.0.1, Sciex) with the Paragon algorithm. The searching was conducted against a revised UniProt Swiss-Prot *Arabidopsis thaliana* protein database (August 2016), specifying iodoacetamide with other possible Cys modifications. The false discovery rate (FDR) was set to 0.01 for both peptides and proteins. The MS/MS spectra of the identified peptides were then used to generate the spectral library for SWATH peak extraction using the add-in for PeakView Software (version 2.1, Sciex) MS/MSALL with SWATH Acquisition MicroApp (version 2.0, Sciex). Peptides with a confidence score above 99% (as obtained from the Protein Pilot database search) were included in the spectral library.

For relative quantitation using SWATH analysis, the same samples used to generate the spectral library were analyzed using a data-independent acquisition (DIA) method. Each sample (2 μL) was analyzed using the LC-MS equipment and LC gradient described above to build the spectral library but instead used the SWATH-MS acquisition method. The method consisted of repeating a cycle that consisted of the acquisition of 34 TOF MS/MS scans (230 to 1500 m/z, 100 ms acquisition time) of overlapping sequential precursor isolation windows of 25 m/z width (1 m/z overlap) covering the 400 to 1250 m/z mass range with a previous TOF MS scan (400 to 1250 m/z, 50 ms acquisition time) for each cycle. The total cycle time was 3.5 s.

The targeted data extraction of the fragment ion chromatogram traces from the SWATH runs was performed by PeakView (version 2.1) with the MS/MSALL with SWATH Acquisition MicroApp (version 2.0). This application processed the data using the spectral library created from the shotgun data. Up to 10 peptides per protein and 7

fragments per peptide were selected, based on signal intensity. Any shared and modified peptides were excluded from the processing. Windows of 12 min and 20 ppm width were used to extract the ion chromatograms. SWATH quantitation was attempted for all proteins in the ion library that were identified by ProteinPilot with an FDR below 1%. The extracted ion chromatograms were then generated for each selected fragment ion. The peak areas for the peptides were obtained by summing the peak areas from the corresponding fragment ions. PeakView computed an FDR and a score for each assigned peptide according to the chromatographic and spectral components. Only peptides with an FDR below 5% were used for protein quantitation. Protein quantitation was calculated by adding the peak areas of the corresponding peptides. To test for differential protein abundance between the two groups, MarkerView (version 1.2.1, Sciex) was used for signal normalization.

The mass spectrometry data have been deposited in the ProteomeXchange Consortium via the PRIDE (Vizcaino et al., 2016) partner repository with the dataset identifier PXD009929.

Expression and purification of recombinant His-tagged proteins

The complementary DNAs encoding the mature chloroplastic SBPase (At3g55800), the mature chloroplastic CYP20-3 (At3g62030), and the complete cytosolic ENO2 (At2g36530) were cloned into the pDEST17 vector (Invitrogen) with Gateway Technology (Invitrogen) to express an N-terminal 6-His-tagged protein using the *Escherichia coli* expression system. For SBPase and ENO2 protein expression, transformed *E. coli* BL21 cell cultures at an optical density at 600 nm of 0.4 were treated with 0.5 mM isopropyl-β-D-thiogalactopyranoside and incubated for an additional 2 h at 37°C. CYP20-3 was also obtained by IPTG induction, but in this case the induction was for 4 h at 30ºC. Purification was performed using nickel resin binding under nondenaturing conditions using a Ni-NTA Purification System (Invitrogen) according to the manufacturer's instructions. Recombinant protein production and purification were assessed by SDS-PAGE using 12% (w/v) polyacrylamide gels and Coomassie brilliant blue staining.

Electrophoretic mobility

Nickel-affinity purified recombinant CYP20-3 was incubated at 4 ºC with potassium cyanide, hydrogen peroxide, DTT or combinations of them for different time

periods and different concentrations as indicated, followed by a further incubation with the alkylating agent 2-iodoacetamide at a concentration of 100 mM for 30 min. Subsequently, 20 µg of the samples were subjected to SDS-PAGE using 15% (w/v) polyacrylamide gels, either under nonreducing or reducing conditions depending on the presence of 2-mercaptoethanol in the loading buffer. After electrophoresis, the proteins were visualized using Coomassie Brilliant Blue staining.

Enzyme activity assays

The PPIase activity of the nickel-affinity purified recombinant CYP20-3 was measured using a chymotrypsin-coupled assay as previously described (Motohashi et al., 2003) with some modifications. An assay mixture containing 44 mM HEPES-NaOH (pH 8.0), 1 µg of the recombinant CYP20-3 and 0.6 mg of chymotrypsin was incubated for 5 min at 1 ºC. To initiate the reaction, 75 µM of the substrate N-succinyl-Ala-Ala-Pro-Phe-p-nitroanilide (Sigma), previously dissolved in trifluoroethanol and LiCl, was added. The absorbance at 367 nm was immediately monitored using UV spectrophotometry for 1.5 min. The specific activities were calculated by using the extinction coefficient of 13.4 mM^{-1} cm^{-1}.

The enolase activity of the nickel-affinity purified recombinant ENO2 was measured using a coupled assay system of lactate dehydrogenase and pyruvate kinase. Enolase activity was monitored as a decrease in NADH absorbance at 340 nm and estimated by using the molar extinction coefficient of NADH of 6.22 mM^{-1} cm^{-1} (Fukano and Kimura, 2014).

In all cases, one unit of activity is defined as the amount of enzyme that catalyzed the production of 1 µmol product min^{-1}.

Accession Numbers

Sequence data from this article can be found in the Web site http://www.arabidopsis.org/ for Arabidopsis genes with locus identifiers provided in this study.

Supplemental Data

The following supplemental materials are available.

Supplemental Dataset 1. Proteins identified by shotgun data dependent acquisition in mitochondrial samples

781 **Supplemental Dataset 2**. Quantified proteins using the SWATH acquisition method in
782 mitochondrial samples
783 **Supplemental Dataset 3**. Identified proteins in ACC treated (R+) and untreated (R-)
784 root samples
785 **Supplemental Table S1.** Overrepresentation test in mitochondrial proteins identified in
786 the spectral library in mitochondrial samples
787 **Supplemental Table S2**. Proteins with different abundance in mitochondrial samples
788 between wild type and *cas-c1* with p value <0.05
789 **Supplemental Table S3.** Identified proteins in the spectral library only present in
790 mitochondrial wild-type samples and absent in *cas-c1*
791 **Supplemental Table S4**. Identified proteins in the spectral library only present in
792 mitochondrial *cas-c1* samples and absent in wild type
793 **Supplemental Table S5**. Functional classification of less abundant or absent proteins in
794 mitochondrial *cas-c1* samples
795 **Supplemental Table S6**. Functional classification of proteins more abundant or only
796 present in mitochondrial *cas-c1* samples
797 **Supplemental Table S7**. Overrepresentation test of the more abundant proteins in
798 mitochondrial *cas-c1* samples
799 **Supplemental Table S8**. S-cyanylated proteins identified in wild-type and *cas-c1*
800 leaves as determined by the chemical 2-imino-thiazolidine method
801 **Supplemental Table S9.** Overrepresentation test of S-cyanylated proteins identified in
802 wild-type and *cas-c1* leaves
803 **Supplemental Table S10.** Total proteins identified as susceptible to S-cyanylation in
804 leaf and root tissues
805 **Supplemental Table S11**. SBPase predicted ion types for S-cyanyl modified peptide.
806 The ions detected in the spectrum are highlighted in red color. This table refers to
807 Figure 4
808 **Supplemental Table S12**. CYP20-3 predicted ion types for the modified peptide. The
809 ions detected in the spectrum are highlighted in red color. This table refers to Figure 5
810 **Supplemental Table S13**. ENO2 predicted ion types for the modified peptide. The ions
811 detected in the spectrum are highlighted in red color. This table refers to Figure 7
812 **Supplemental Figure S1**. Schematic image of the signaling pathway and components
813 involved in biotic stress that are absent or less abundant in mitochondrial *cas-c1*
814 samples. A) Blue squares represent proteins classified in biotic stress according to GO

classification by Mapman. B) Proteins classified as membrane bound receptor kinases according to GO classification by Mapman. Blue squares indicate those identified by our analysis.

Supplemental Figure S2. Representative diagram of the Calvin cycle (A) and the glycolysis pathway (B) with the proteins identified as S-cyanylated in leaf and root tissues. S- cyanylated proteins are shown as names or AGI locus in black color

ACKNOWLEDGMENTS

We thank the European Regional Development Fund through the Agencia Estatal de Investigación grant BIO2016-76633-P for financial support. L. A-A. was supported by the Ministerio de Economia y Competitividad through the program of Formación de Personal Investigador. We also thanks Rocio Rodríguez from the Proteomic Facility at IBVF, Angeles Aroca, and Ignacio Ortea from IMIBIC for their technical advice.

Table 1. S-cyanylated proteins and peptides identified in total protein extracts from root tissues by untargeted LC-MS/MS analysis.

AGI locus	Description	S-Cyanylated peptide
At1g07890	Ascorbate peroxidase APX1	GLIAEKNCAPIMVR
At1g12820	Auxin signaling F-box 3 protein AFB3	SLWMSSCEVTLGGCK (2 Cyano)
At1g15890	Disease resistance protein (CC-NBS-LRR class) family	QKETLCVK
At1g35720	Member of the annexin gene family ANN1	STIQCLTRPELYFVDVLR
At1g52150	Homeobox-leucine zipper protein AtHB-15	ECPILSNIEPK
At1g53310	Phosphoenolpyruvate carboxylase PPC1	SLCSCGDRPIADGSLLDFLR
At1g54340	NADP-specific isocitrate dehydrogenase ICDH	LVPGWTKPICIGR
At1g60810	ATP-citrate lyase ACLA-2	LGCSISFSECGGIDIEENWDKVK
At1g64190	6-phosphogluconate dehydrogenase PGD1	ICSYAQGMNLLR
At1g65930	Cytosolic isocitrate dehydrogenase [NADP]	CATITPDEGRVTEFGLK
		CATITPDEGR
		LVPGWTKPICIGR
At2g01520	MLP328	IWNYTCDGKPEVFK
At2g01530	MLP329	IWNYTCDGKPEVFK
At2g17360	40S ribosomal protein S4-1	SRECLPLVLIIR
At2g17420	NADPH-dependent thioredoxin reductase NTR2	VCIVGSGPAAHTAAIYASR
At2g20420	ATP citrate lyase (ACL) family protein	CDVIASGIVNAAK
At2g21660	Small glycine-rich RNA binding protein CCR2	CFVGGLAWATDDR
At2g31610	40S ribosomal protein S3-1	GLCAIAQAESLR
At2g34220	Maternal effect embryo arrest 20, MEE20	CFLSVVR
At2g36530	Enolase ENO2/LOS2	SCNALLLK
At2g45290	Transketolase TKL2	NLSQQCLNALAK
At2g48060	piezo-type mechanosensitive ion channel component	VECRMNQLLR
At3g02360	6-phosphogluconate dehydrogenase PGD2	ICSYAQGMNLIR
At3g03670	Peroxidase superfamily protein	MHFHDCFVQGCDASLLIDPTTSQLSEK
At3g03780	Methionine synthase MS2	CVKPPVIYGDVSRPK
At3g05590	60S ribosomal protein RPL18	AGGECLTFDQLALR
At3g11670	Digalactosyldiacylglycerol synthase 1	AYCDKVLR
At3g19390	Granulin repeat cysteine protease family protein	CGVAMMASYPTK
At3g22860	Eukaryotic translation initiation factor 3 subunit C	AMLCDIYQHALMDNFVTAR
At3g23600	Alpha/beta-hydrolases superfamily protein	SGPQCCENPPTLNPVSGSGHVEK
At3g23810	S-adenosyl-l-homocysteine hydrolase ATSAHH2	VAVICGYGDVGK
At3g27430	20S proteasome beta subunit PBB1	TEGPIVADKNCEKIHYMAPNIYCCGA
		GTAADTEAVTDMVSSQLR
At3g32980	Peroxidase family protein	TVSCADILTIAAQQAVNLAGGPSWR
At3g48340	KDEL-tailed cysteine endopeptidase CEP2	CGIAMEASYPIK
At3g48990	4-coumarate-CoA ligase-like 10	SCSASLAPVILSR
At3g53870	40S ribosomal protein S3-2	GLCAIAQAESLR
At3g57610	Adenylosuccinate synthetase (AdSS)	CQGGANAGHTIYNSEGKK
At3g60750	Transketolase ATTKL1	NLSQQCLNALAK
		SGHPGLPMGCAPMAHILYDEVMR
At4g13930	Serine hydroxymethyltransferase SHM4	LLICGGSAYPR
At4g13940	S-adenosyl-L-homocysteine hydrolase HOG1	VAVICGYGDVGK
At4g14140	DNA methyltransferase DMT2	CGIAMEASYPIK
At4g22970	Separase-like protein ESP/RSW4	CAVSLVR
At4g26970	Aconitase ACO2	SFVCTLRFDTEVELAYYDHGGILPYVIR
At4g34870	Rotamase cyclophilin CYP18-4/ROC5	VIPGFMCQGGDFTAK
At4g35830	Aconitase ACO1	SFTCTLRFDTEVELAYFDHGGILQYVIR
At5g07660	Structural maintenance of chromosomes protein 6A	ERVPTCQNKIDR
At5g11670	NADP-dependent malic enzyme NADP-ME2	TYLPGQANNCYIFPGLGLGLIMSGAIR
At5g11920	Protein with fructan exohydrolase activity	CLIDHSIIESYGVGGK
At5g12080	Mechanosensitive ion channel ATMSL10	VLKCITR

890	At5g14590	Isocitrate dehydrogenase	CATITPDEGR
891	At5g16210	HEAT repeat-containing protein	IIMDACVSLSR
892	At5g17920	Methionine synthase ATMS1	CVKPPVIYGDVSRPK
893	At5g20160	Ribosomal protein L7Ae/L30e/S12e/Gadd45	ACGVTRPVIACSVTSNEASQLK
894	At5g27850	60S ribosomal protein L18-3	AGGECLTFDQLALR
895	At5g35530	40S ribosomal protein S3-3	GLCAIAQAESLR
896	At5g40580	20S proteasome beta subunit PBB2A	TEGPIVADKNCEKIHYMAPNIY
897			CCGAGTAADTEAVTDMVSSQLR
898	At5g41670	6-phosphogluconate dehydrogenasePGD3	ICSYAQGMNLLR
899	At5g43060	Cysteine protease family protein RD21B	CGIAMEASYPIKK
900	At5g45500	RNI-like superfamily protein	CKVTVLR
901	At5g46850	Phosphatidylinositol-glycan biosynthesis	RCLVLSIGR
902	At5g52640	Heat shock protein AtHsp90-1	VVVSDRIVDSPCCLVTGEYGWTANMER
903			(2 Cyano)
904	At5g56000	Heat shock protein AtHsp90-4 / Hsp81-4	VIVSDRVVDSPCCLVTGEYGWTANMER
905			(2 Cyano)
906	At5g56010	Heat shock protein AtHsp90-3 / Hsp81-3	VIVSDRVVDSPCCLVTGEYGWTANMER
907			(2 cyano)
908	At5g56030	Heat shock protein AtHsp90-2 / Hsp81-3 / ERD8	VIVSDRVVDSPCCLVTGEYGWTANMER
909			(2 cyano)
910	At5g58420	40S ribosomal protein RPS4A	SRECLPLVLIIR
911			
912			
913			

Figure legends

Figure 1. Protein-protein interaction network of the abundant proteins in mitochondrial *cas-c1* samples. Round nodes represent proteins, and lines represent interactions. Dashed lines represent inter-cluster edges. Node modules indicated in red, yellow, blue and green were identified by *k*-means clustering.

Figure 2. Cyanylation and *in vitro* analysis in leaf samples. A) Chemical cleavage of the peptide chains on the N-terminal side of cyanylated cysteine residues. S-cyanylated peptide at alkaline pH results in the cleavage of the protein into two peptides: the N-terminal backbone at the Cys-CN residue and a cycled iminothiazoline derivative peptide. B) Representative 2D IEF-SDS PAGE protein profile of protein extracts of 2-week-old Arabidopsis *cas-c1* mutant leaves treated with 100 µM ACC for 24 h. Proteins were treated with 0.01 M NaOH (control samples) or 1 M NH_4OH and were separated in the first dimension in gel strips (7 cm) with a linear pH gradient 4–7 and in 12% acrylamide vertical gels in the second dimension and stained with Coomassie-blue G-250. White circles show the mobility shift of a representative protein (SBPase).

Figure 3. Protein-protein interaction network of identified S-cyanylated proteins in leaf and root tissues. Round nodes represent proteins, and lines edges represent interactions. Dashed lines represent inter-cluster edges. Node modules indicated in red, yellow, blue and green were identified by *k*-means clustering.

Figure 4. Identification of sedoheptulose 1, 7-bisphosphatase using mass spectrometry. (A) The protein was identified with a sequence coverage of 67%. The identified peptides are shown in red and the peptide containing S-cyanylated Cys^{74} is underlined. The modified Cys residue is shown in blue color. (B) Mass spectrum from the LC-MS/MS analysis of the tryptic peptide containing Cys^{74} of SBPase. Predicted ion types and the detected ions are shown in Table S11.

Figure 5. Identification of peptidyl-prolyl cis-trans isomerase CYP20-3 using mass spectrometry. (A) The protein was identified with a sequence coverage of 61%. The identified peptides are shown in red, and the peptide containing S-cyanylated Cys^{206} is underlined. The modified Cys residue is shown in blue color. (B) Mass spectrum from

948 the LC-MS/MS analysis of the tryptic peptide containing Cys^{206} of CYP20-3. Predicted
949 ion types and the detected ions are shown in Table S12.
950
951 **Figure 6. Protein mobility shift and enzymatic activity assays of CYP20-3.** (A)
952 Alkylation of purified CYP20-3 protein without any treatment (-); after a 20 min
953 treatment with 0.1 mM DTT (+DTT); after a sequential treatment of 20 min with 0.1
954 mM DTT and 20 additional min with 1 mM KCN (+DTT+KCN); after a treatment of
955 20 min 0.1 mM H_2O_2 (+H_2O_2); or after a sequential treatment of 20 min 0.1 mM H_2O_2
956 and additional 20 min with 1 mM KCN (+H_2O_2+KCN). The first lane (+ß-ME)
957 corresponds to the non-alkylated, ß-mercaptoethanol-reduced protein. MW, molecular
958 weight markers. Reduced (red) and oxidized (ox) forms are indicated. (B) Enzymatic
959 activity of purified CYP20-3 protein without any treatment (-); after a 20 min treatment
960 with 0.1 mM H_2O_2 (+H_2O_2); after a sequential treatment of 20 min with 0.1 mM H_2O_2
961 and 20 additional min with 1 mM KCN (+H_2O_2+KCN); or after a sequential treatment
962 of 20 min with 0.1 mM H_2O_2, 20 additional min with 1 mM KCN (+H_2O_2+KCN) and
963 20 additional min with 10 mM DTT (+H_2O_2+KCN+DTT). All results are shown as the
964 mean ± SD (n = 3). a, Significant differences with control sample ($P < 0.05$, one-way
965 ANOVA).
966
967 **Figure 7. Identification of enolase ENO2 using mass spectrometry.** (A) The protein
968 was identified with a sequence coverage of 64%. The peptides identified are shown in
969 red, and the peptide containing S-cyanylated Cys^{346} is underlined. The modified Cys
970 residue is shown in blue color. (B) Mass spectrum from LC-MS/MS analysis of the
971 tryptic peptide containing the Cys^{346} of ENO2. Predicted ion types and the detected ions
972 are shown in Table S13.
973
974 **Figure 8. Enzymatic assay of ENO2**. Enolase activity of purified ENO2 protein
975 without any treatment (-), after a 20 min treatment with 0.1 mM H_2O_2 (+H_2O_2), or after
976 a sequential treatment of 20 min with 0.1 mM H_2O_2 and 20 additional min with 1 mM
977 KCN (+H_2O_2+KCN). All results are shown as the mean ± SD (n = 6). a, Significant
978 differences with control sample ($P < 0.05$, one-way ANOVA).
979
980 **Figure 9. Schematic representation of significant metabolic pathways regulated by**
981 **S-cyanylation.** Red stars mark proteins that can be posttranslationally modified by

hydrogen cyanide. The number inside the red star at the Calvin cycle represents the number of proteins. TCA, tricarboxylic acid cycle; ETC/OXOPHOS, electron transport chain and oxidative phosphorylation; SAM, S-adenosyl methionine; SAH, S-adenosyl homocysteine.

LITERATURE CITED

Alvarez, C., García, I., Romero, L.C., Gotor, C. (2012). Mitochondrial Sulfide Detoxification Requires a Functional Isoform O-Acetylserine(thiol)lyase C in Arabidopsis thaliana. Mol Plant **5:** 1217-1226.

Alvarez, C., Lozano-Juste, J., Romero, L.C., Garcia, I., Gotor, C., Leon, J. (2011). Inhibition of Arabidopsis O-acetylserine(thiol)lyase A1 by tyrosine nitration. J Biol Chem **286:** 578-586.

Anderson, L.E., Li, A.D., Stevens, F.J. (1998). The enolases of ice plant and Arabidopsis contain a potential disulphide and are redox sensitive. Phytochemistry **47:** 707-713.

Arenas-Alfonseca, L., Gotor, C., Romero, L.C., Garcia, I. (2018). ß-Cyanoalanine Synthase Action in Root Hair Elongation is Exerted at Early Steps of the Root Hair Elongation Pathway and is Independent of Direct Cyanide Inactivation of NADPH Oxidase. Plant Cell Physiol **59:** 1072-1083.

Aroca, A., Gotor, C., Romero, L.C. (2018). Hydrogen Sulfide Signaling in Plants: Emerging Roles of Protein Persulfidation. Front Plant Sci **9**.

Aroca, A., Benito, J.M., Gotor, C., Romero, L.C. (2017a). Persulfidation proteome reveals the regulation of protein function by hydrogen sulfide in diverse biological processes in Arabidopsis. J Exp Bot **68:** 4915-4927.

Aroca, A., Schneider, M., Scheibe, R., Gotor, C., Romero, L.C. (2017b). Hydrogen Sulfide Regulates the Cytosolic/Nuclear Partitioning of Glyceraldehyde-3-Phosphate Dehydrogenase by Enhancing its Nuclear Localization. Plant Cell Physiol **58:** 983-992.

Aroca, Á., Serna, A., Gotor, C., Romero, L.C. (2015). S-Sulfhydration: A Cysteine Posttranslational Modification in Plant Systems. Plant Physiol **168:** 334-342.

Baskar, V., Park, S.W., Nile, S.H. (2016). An Update on Potential Perspectives of Glucosinolates on Protection against Microbial Pathogens and Endocrine Dysfunctions in Humans. Crit Rev Food Sci Nutr **56:** 2231-2249.

Berg, S.P., Krogmann, D.W. (1975). Mechanism of KCN inhibition of photosystem I. J Biol Chem **250:** 8957-8962.

Bermudez, M.A., Paez-Ochoa, M.A., Gotor, C., Romero, L.C. (2010). Arabidopsis S-sulfocysteine synthase activity is essential for chloroplast function and long-day light-dependent redox control. Plant Cell **22:** 403-416.

Bermudez, M.A., Galmes, J., Moreno, I., Mullineaux, P.M., Gotor, C., Romero, L.C. (2012). Photosynthetic adaptation to length of day is dependent on S-sulfocysteine synthase activity in the thylakoid lumen. Plant Physiol **160:** 274-288.

Bethke, P.C., Libourel, L.G.L., Reinohl, V., Jones, R.L. (2006). Sodium nitroprusside, cyanide, nitrite, and nitrate break Arabidopsis seed dormancy in a nitric oxide-dependent manner. Planta **223:** 805-812.

Bishop, N.I., Spikes, J.D. (1955). Inhibition by Cyanide of the Photochemical Activity of Isolated Chloroplasts. Nature **176:** 307-308.

Bottcher, C., Westphal, L., Schmotz, C., Prade, E., Scheel, D., Glawischnig, E. (2009). The multifunctional enzyme CYP71B15 (PHYTOALEXIN DEFICIENT3) converts cysteine-indole-3-acetonitrile to camalexin in the indole-3-acetonitrile metabolic network of Arabidopsis thaliana. Plant Cell **21:** 1830-1845.

Boukouris, A.E., Zervopoulos, S.D., Michelakis, E.D. (2016). Metabolic Enzymes Moonlighting in the Nucleus: Metabolic Regulation of Gene Transcription. Trends Biochem Sci **41:** 712-730.

Buchanan, B.B., Balmer, Y. (2005). Redox regulation: a broadening horizon. Annu Rev Plant Biol **56:** 187-220.

Catsimpoolas, N., Wood, J.L. (1966). Specific cleavage of cystine peptides by cyanide. J Biol Chem **241:** 1790-1796.

Chen, Z. (2001). A superfamily of proteins with novel cysteine-rich repeats. Plant Physiol **126:** 473-476.

Chivasa, S., Carr, J.P. (1998). Cyanide restores N gene-mediated resistance to tobacco mosaic virus in transgenic tobacco expressing salicylic acid hydroxylase. Plant Cell **10:** 1489-1498.

Cohen, W.S., McCarty, R.E. (1976). Reversibility of the cyanide inhibition of electron transport in spinach chloroplast thylakoids. Biochem Biophys Res Commun **73:** 679-685.

Eremina, M., Rozhon, W., Yang, S., Poppenberger, B. (2015). ENO2 activity is required for the development and reproductive success of plants, and is feedback-repressed by AtMBP-1. Plant J **81:** 895-906.

Fasco, M.J., Iii, C.R., Stack, R.F., O'Hehir, C., Barr, J.R., Eadon, G.A. (2007). Cyanide adducts with human plasma proteins: albumin as a potential exposure surrogate. Chem Res Toxicol **20:** 677-684.

Fricker, L.D. (2015). Limitations of Mass Spectrometry-Based Peptidomic Approaches. J Am Soc Mass Spectrom **26:** 1981-1991.

Fukano, K., Kimura, K. (2014). Measurement of enolase activity in cell lysates. Methods Enzymol **542:** 115-124.

Garcia, I., Gotor, C., Romero, L.C. (2014). Beyond toxicity: A regulatory role for mitochondrial cyanide. Plant Signal Behav **9:** e27612.

Garcia, I., Rosas, T., Bejarano, E.R., Gotor, C., Romero, L.C. (2013). Transient transcriptional regulation of the CYS-C1 gene and cyanide accumulation upon pathogen infection in the plant immune response. Plant Physiol **162:** 2015-2027.

Garcia, I., Castellano, J.M., Vioque, B., Solano, R., Gotor, C., Romero, L.C. (2010). Mitochondrial beta-cyanoalanine synthase is essential for root hair formation in Arabidopsis thaliana. Plant Cell **22:** 3268-3279.

Gawron, O. (1966). CHAPTER 14 - ON THE REACTION OF CYANIDE WITH CYSTINE AND CYSTINE PEPTIDES. In The Chemistry of Organic Sulfur Compounds (Pergamon), pp. 351-365.

Geigenberger, P., Kolbe, A., Tiessen, A. (2005). Redox regulation of carbon storage and partitioning in response to light and sugars. J Exp Bot **56:** 1469-1479.

Giege, P., Heazlewood, J.L., Roessner-Tunali, U., Millar, A.H., Fernie, A.R., Leaver, C.J., Sweetlove, L.J. (2003). Enzymes of glycolysis are functionally

associated with the mitochondrion in Arabidopsis cells. Plant Cell **15:** 2140-2151.

Gotor, C., Laureano-Marín, A.M., Arenas-Alfonseca, L., Moreno, I., Aroca, Á., García, I., Romero, L.C. (2017). Advances in Plant Sulfur Metabolism and Signaling. In Progress in Botany Vol. 78, F M Cánovas, U Lüttge,R Matyssek, eds (Cham: Springer International Publishing), pp. 45-66.

Grierson, C., Nielsen, E., Ketelaarc, T., Schiefelbein, J. (2014). Root hairs. Arabidopsis Book **12:** e0172.

Grigoryan, H., Edmands, W., Lu, S.S., Yano, Y., Regazzoni, L., Iavarone, A.T., Williams, E.R., Rappaport, S.M. (2016). Adductomics Pipeline for Untargeted Analysis of Modifications to Cys34 of Human Serum Albumin. Anal Chem **88:** 10504-10512.

Hanschen, F.S., Lamy, E., Schreiner, M., Rohn, S. (2014). Reactivity and stability of glucosinolates and their breakdown products in foods. Angew Chem Int Ed Engl **53:** 11430-11450.

Harmel, R., Fiedler, D. (2018). Features and regulation of non-enzymatic post-translational modifications. Nat Chem Biol **14:** 244.

Hatzfeld, Y., Maruyama, A., Schmidt, A., Noji, M., Ishizawa, K., Saito, K. (2000). beta-Cyanoalanine synthase is a mitochondrial cysteine synthase-like protein in spinach and Arabidopsis. Plant Physiol **123:** 1163-1171.

Holtgrefe, S., Gohlke, J., Starmann, J., Druce, S., Klocke, S., Altmann, B., Wojtera, J., Lindermayr, C., Scheibe, R. (2008). Regulation of plant cytosolic glyceraldehyde 3-phosphate dehydrogenase isoforms by thiol modifications. Physiol Plant **133:** 211-228.

Isom, G.E., Way, J.L. (1984). Effects of oxygen on the antagonism of cyanide intoxication: cytochrome oxidase, in vitro. Toxicol Appl Pharmacol **74:** 57-62.

Jacobson, G.R., Schaffer, M.H., Stark, G.R., Vanaman, T.C. (1973). Specific chemical cleavage in high yield at the amino peptide bonds of cysteine and cystine residues. J Biol Chem **248:** 6583-6591.

Jeong, J.S., Jung, C., Seo, J.S., Kim, J.K., Chua, N.H. (2017). The Deubiquitinating Enzymes UBP12 and UBP13 Positively Regulate MYC2 Levels in Jasmonate Responses. Plant Cell **29:** 1406-1424.

Klie, S., Nikoloski, Z. (2012). The Choice between MapMan and Gene Ontology for Automated Gene Function Prediction in Plant Science. Front Genet **3:** 115.

Knowles, C.J. (1976). Microorganisms and cyanide. Bacteriol Rev **40:** 652-680.

Laemmli, U.K. (1970). Cleavage of structural proteins during the assembly of the head of bacteriophage T4. Nature **227:** 680-685.

Lee, H., Guo, Y., Ohta, M., Xiong, L., Stevenson, B., Zhu, J.K. (2002). LOS2, a genetic locus required for cold-responsive gene transcription encodes a bi-functional enolase. EMBO J **21:** 2692-2702.

Lee, S., Doxey, A.C., McConkey, B.J., Moffatt, B.A. (2012). Nuclear targeting of methyl-recycling enzymes in Arabidopsis thaliana is mediated by specific protein interactions. Mol Plant **5:** 231-248.

Lozano-Durán, R., García, I., Huguet, S., Balzergue, S., Romero, L.C., Bejarano, E.R. (2012). Geminivirus C2 protein represses genes involved in sulphur assimilation and this effect can be counteracted by jasmonate treatment. Eur J Plant Pathol **134:** 49-59.

Mi, H., Huang, X., Muruganujan, A., Tang, H., Mills, C., Kang, D., Thomas, P.D. (2017). PANTHER version 11: expanded annotation data from Gene Ontology

and Reactome pathways, and data analysis tool enhancements. Nucleic Acids Res **45:** D183-d189.

Moller, I.M., Rogowska-Wrzesinska, A., Rao, R.S. (2011). Protein carbonylation and metal-catalyzed protein oxidation in a cellular perspective. J Proteomics **74:** 2228-2242.

Monaghan, J., Xu, F., Gao, M., Zhao, Q., Palma, K., Long, C., Chen, S., Zhang, Y., Li, X. (2009). Two Prp19-like U-box proteins in the MOS4-associated complex play redundant roles in plant innate immunity. PLoS Pathog **5:** e1000526.

Motohashi, K., Koyama, F., Nakanishi, Y., Ueoka-Nakanishi, H., Hisabori, T. (2003). Chloroplast cyclophilin is a target protein of thioredoxin. Thiol modulation of the peptidyl-prolyl cis-trans isomerase activity. J Biol Chem **278:** 31848-31852.

Nguema-Ona, E., Bannigan, A., Chevalier, L., Baskin, T.I., Driouich, A. (2007). Disruption of arabinogalactan proteins disorganizes cortical microtubules in the root of Arabidopsis thaliana. Plant J **52:** 240-251.

Nicholls, P., Marshall, D.C., Cooper, C.E., Wilson, M.T. (2013). Sulfide inhibition of and metabolism by cytochrome c oxidase. Biochem Soc Trans **41:** 1312-1316.

Ortea, I., Ruiz-Sanchez, I., Canete, R., Caballero-Villarraso, J., Canete, M.D. (2018). Identification of candidate serum biomarkers of childhood-onset growth hormone deficiency using SWATH-MS and feature selection. J Proteomics **175:** 105-113.

Park, C.-M., Weerasinghe, L., Day, J.J., Fukuto, J.M., Xian, M. (2015). Persulfides: Current Knowledge and Challenges in Chemistry and Chemical Biology. Molecular bioSystems **11:** 1775-1785.

Peiser, G.D., Wang, T.T., Hoffman, N.E., Yang, S.F., Liu, H.W., Walsh, C.T. (1984). Formation of cyanide from carbon 1 of 1-aminocyclopropane-1-carboxylic acid during its conversion to ethylene. Proc Natl Acad Sci U S A **81:** 3059-3063.

Rao, R.S.P., Salvato, F., Thal, B., Eubel, H., Thelen, J.J., Møller, I.M. (2017). The proteome of higher plant mitochondria. Mitochondrion **33:** 22-37.

Ressler, C., Giza, Y.H., Nigam, S.N. (1969). ß-Cyanoalanine, product of cyanide fixation and intermediate in asparagine biosynthesis in certain species of Lathyrus and Vicia. J Am Chem Soc **91:** 2766-2775.

Rocha, P.S., Sheikh, M., Melchiorre, R., Fagard, M., Boutet, S., Loach, R., Moffatt, B., Wagner, C., Vaucheret, H., Furner, I. (2005). The Arabidopsis HOMOLOGY-DEPENDENT GENE SILENCING1 gene codes for an S-adenosyl-L-homocysteine hydrolase required for DNA methylation-dependent gene silencing. Plant Cell **17:** 404-417.

Romero, L.C., Aroca, M.A., Laureano-Marin, A.M., Moreno, I., Garcia, I., Gotor, C. (2014). Cysteine and cysteine-related signaling pathways in Arabidopsis thaliana. Mol Plant **7:** 264-276.

Salvato, F., Havelund, J.F., Chen, M., Rao, R.S.P., Rogowska-Wrzesinska, A., Jensen, O.N., Gang, D.R., Thelen, J.J., Møller, I.M. (2014). The Potato Tuber Mitochondrial Proteome. Plant Physiol **164:** 637-653.

Sauter, M., Moffatt, B., Saechao, M.C., Hell, R., Wirtz, M. (2013). Methionine salvage and S-adenosylmethionine: essential links between sulfur, ethylene and polyamine biosynthesis. Biochem J **451:** 145-154.

Seo, S., Mitsuhara, I., Feng, J., Iwai, T., Hasegawa, M., Ohashi, Y. (2011). Cyanide, a coproduct of plant hormone ethylene biosynthesis, contributes to the resistance of rice to blast fungus. Plant Physiol **155:** 502-514.

Struglics, A., Fredlund, K.M., Rasmusson, A.G., Møller, I.M. (1993). The presence of a short redox chain in the membrane of intact potato tuber peroxisomes and the association of malate dehydrogenase with the peroxisomal membrane. Physiol Plant **88:** 19-28.

Szklarczyk, D., Morris, J.H., Cook, H., Kuhn, M., Wyder, S., Simonovic, M., Santos, A., Doncheva, N.T., Roth, A., Bork, P., Jensen, L.J., von Mering, C. (2017). The STRING database in 2017: quality-controlled protein-protein association networks, made broadly accessible. Nucleic Acids Res **45:** D362-d368.

Szklarczyk, D., Franceschini, A., Wyder, S., Forslund, K., Heller, D., Huerta-Cepas, J., Simonovic, M., Roth, A., Santos, A., Tsafou, K.P., Kuhn, M., Bork, P., Jensen, L.J., von Mering, C. (2015). STRING v10: protein-protein interaction networks, integrated over the tree of life. Nucleic Acids Res **43:** D447-452.

Tang, D., Wang, G., Zhou, J.-M. (2017). Receptor Kinases in Plant-Pathogen Interactions: More Than Pattern Recognition. The Plant Cell **29:** 618-637.

Taylorson, R.B., Hendricks, S.B. (1973). Promotion of seed germination by cyanide. Plant Physiol **52:** 23-27.

Thimm, O., Blasing, O., Gibon, Y., Nagel, A., Meyer, S., Kruger, P., Selbig, J., Muller, L.A., Rhee, S.Y., Stitt, M. (2004). MAPMAN: a user-driven tool to display genomics data sets onto diagrams of metabolic pathways and other biological processes. Plant J **37:** 914-939.

Thompson, J.P., Marrs, T.C. (2012). Hydroxocobalamin in cyanide poisoning. Clinical toxicology (Philadelphia, Pa **50:** 875-885.

Tinajero-Trejo, M., Jesse, H.E., Poole, R.K. (2013). Gasotransmitters, poisons, and antimicrobials: it's a gas, gas, gas! F1000Prime Rep **5:** 28.

Trebst, A.V., Losada, M., Arnon, D.I. (1960). Photosynthesis by isolated chloroplasts. XII. Inhibitors of carbon dioxide assimilation in a reconstituted chloroplast system. J Biol Chem **235:** 840-844.

Vizcaino, J.A., Csordas, A., del-Toro, N., Dianes, J.A., Griss, J., Lavidas, I., Mayer, G., Perez-Riverol, Y., Reisinger, F., Ternent, T., Xu, Q.W., Wang, R., Hermjakob, H. (2016). 2016 update of the PRIDE database and its related tools. Nucleic Acids Res **44:** D447-456.

Vowinckel, J., Capuano, F., Campbell, K., Deery, M.J., Lilley, K.S., Ralser, M. (2013). The beauty of being (label)-free: sample preparation methods for SWATH-MS and next-generation targeted proteomics. F1000Res **2:** 272.

Wagner, E.S., Davis, R.E. (1966). Displacement Reactions. IX. The Reaction of Cyanide Ion with Cystine. An Example of Amino Group Participation as Detected with Nitrogen-15 during Cleavage of a Sulfur-Sulfur Bond1. J Am Chem Soc **88:** 7-12.

Wang, R. (2014). Gasotransmitters: growing pains and joys. Trends Biochem Sci **39:** 227-232.

Williams, S.J., Sohn, K.H., Wan, L., Bernoux, M., Sarris, P.F., Segonzac, C., Ve, T., Ma, Y., Saucet, S.B., Ericsson, D.J., Casey, L.W., Lonhienne, T., Winzor, D.J., Zhang, X., Coerdt, A., Parker, J.E., Dodds, P.N., Kobe, B., Jones, J.D. (2014). Structural basis for assembly and function of a heterodimeric plant immune receptor. Science **344:** 299-303.

Wong, C.E., Carson, R.A., Carr, J.P. (2002). Chemically induced virus resistance in Arabidopsis thaliana is independent of pathogenesis-related protein expression and the NPR1 gene. Mol Plant Microbe Interact **15:** 75-81.

Wu, J., Watson, J.T. (1998). Optimization of the cleavage reaction for cyanylated cysteinyl proteins for efficient and simplified mass mapping. Anal Biochem **258:** 268-276.

Wu, X., Li, F., Kolenovsky, A., Caplan, A., Cui, Y., Cutler, A., Tsang, E.W.T. (2009). A mutant deficient in S-adenosylhomocysteine hydrolase in Arabidopsis shows defects in root-hair developmentThis paper is one of a selection of papers published in a Special Issue from the National Research Council of Canada – Plant Biotechnology Institute. Botany **87:** 571-584.

Yamasaki, H., Watanabe, N.S., Sakihama, Y., Cohen, M.F. (2016). An Overview of Methods in Plant Nitric Oxide (NO) Research: Why Do We Always Need to Use Multiple Methods? Methods Mol Biol **1424:** 1-14.

Yip, W.K., Yang, S.F. (1988). Cyanide metabolism in relation to ethylene production in plant tissues. Plant Physiol **88:** 473-476.

Zaffagnini, M., Fermani, S., Costa, A., Lemaire, S.D., Trost, P. (2013). Plant cytoplasmic GAPDH: redox post-translational modifications and moonlighting properties. Front Plant Sci **4:** 450.

Zhang, D., Macinkovic, I., Devarie-Baez, N.O., Pan, J., Park, C.M., Carroll, K.S., Filipovic, M.R., Xian, M. (2014). Detection of protein S-sulfhydration by a tag-switch technique. Angew Chem Int Ed Engl **53:** 575-581.

Zidenga, T., Siritunga, D., Sayre, R.T. (2017). Cyanogen Metabolism in Cassava Roots: Impact on Protein Synthesis and Root Development. Front Plant Sci **8:** 220.

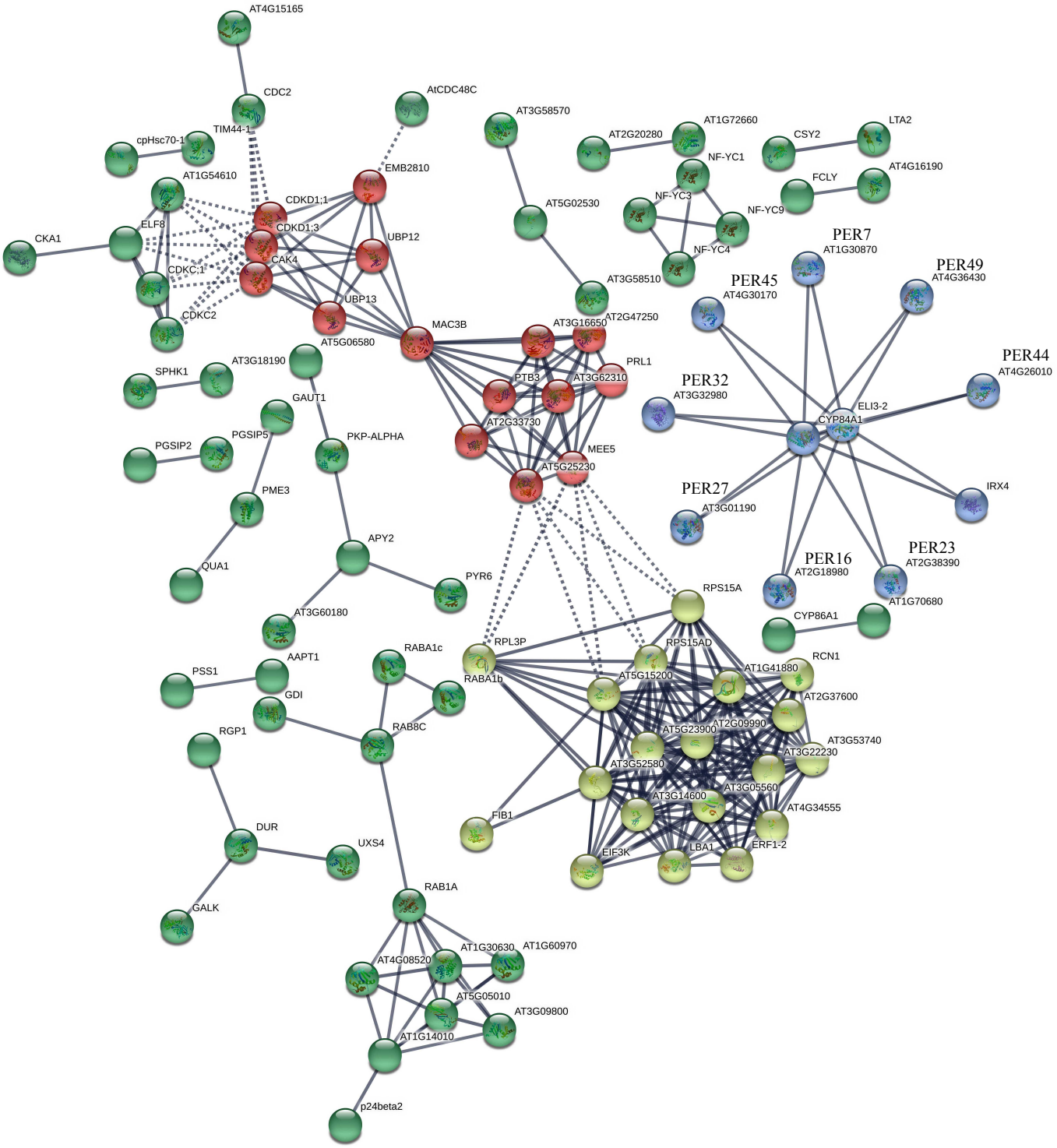

Figure 1. Protein-protein interaction network of the abundant proteins in mitochondrial *cas-c1* samples . Round nodes represents proteins, and lines represent interactions. Dashed lines represent inter-cluster edges. Node modules indicated in red, yellow, blue and green colors were identified by *k*-means clustering

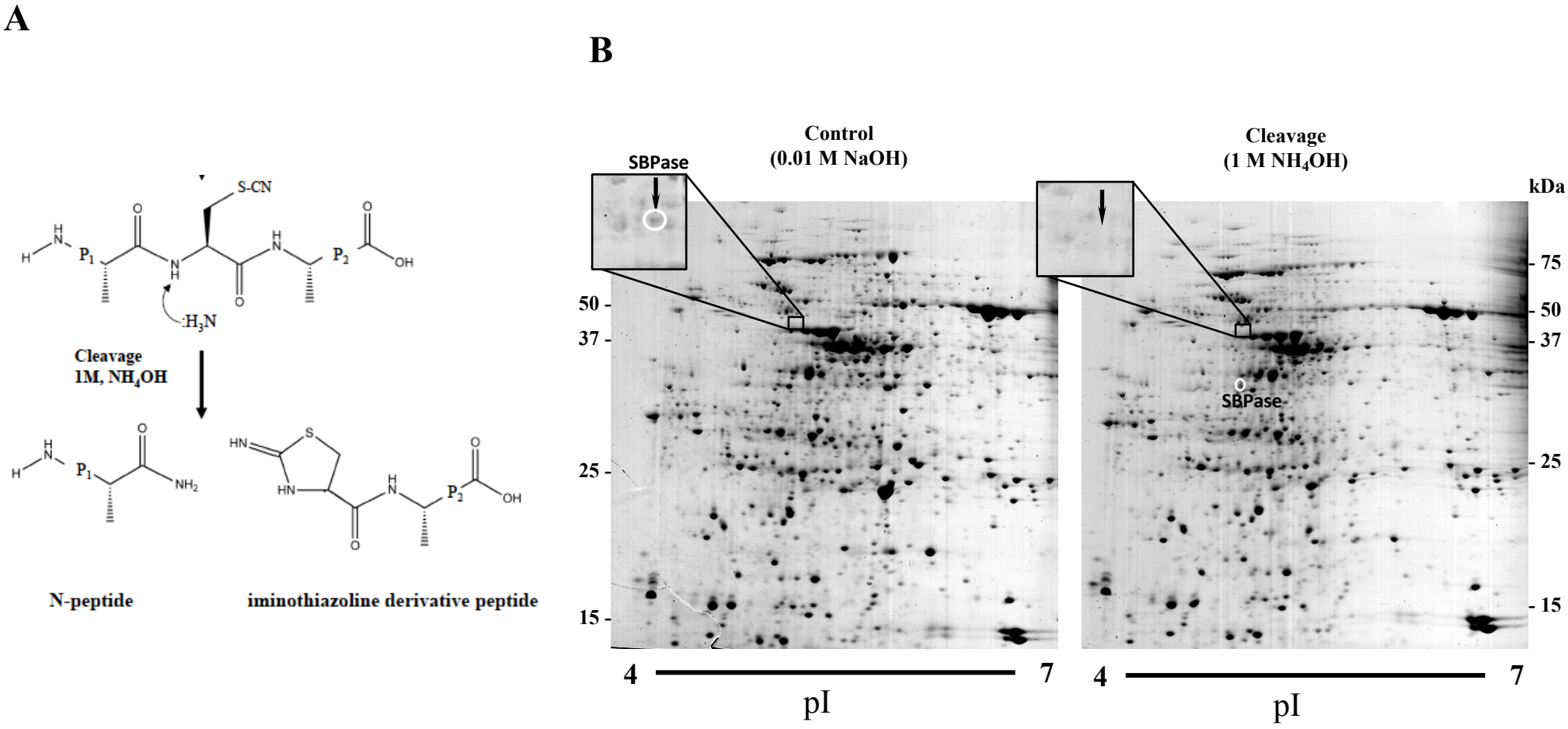

Figure 2. Cyanylation and *in vitro* analysis in leaf samples. A) Chemical cleavage of the peptide chains on the N-terminal side of cyanylated cysteine residues. S-cyanylated peptide at alkaline pH results in the cleavage of the protein into two peptides: the N-terminal backbone at the Cys-CN residue and a cycled iminothiazoline derivative peptide. B) Representative 2D IEF-SDS PAGE protein profile of protein extracts of 2-week-old Arabidopsis *cas-c1* mutant leaves treated with 100 µM ACC for 24 h. Proteins were treated with 0.01 M NaOH (control samples) or 1 M NH_4OH and were separated in the first dimension in gel strips (7 cm) with a linear pH gradient 4–7 and in 12% acrylamide vertical gels in the second dimension and stained with Coomassie-blue G-250. White circles show the mobility shift of a representative protein (SBPase).

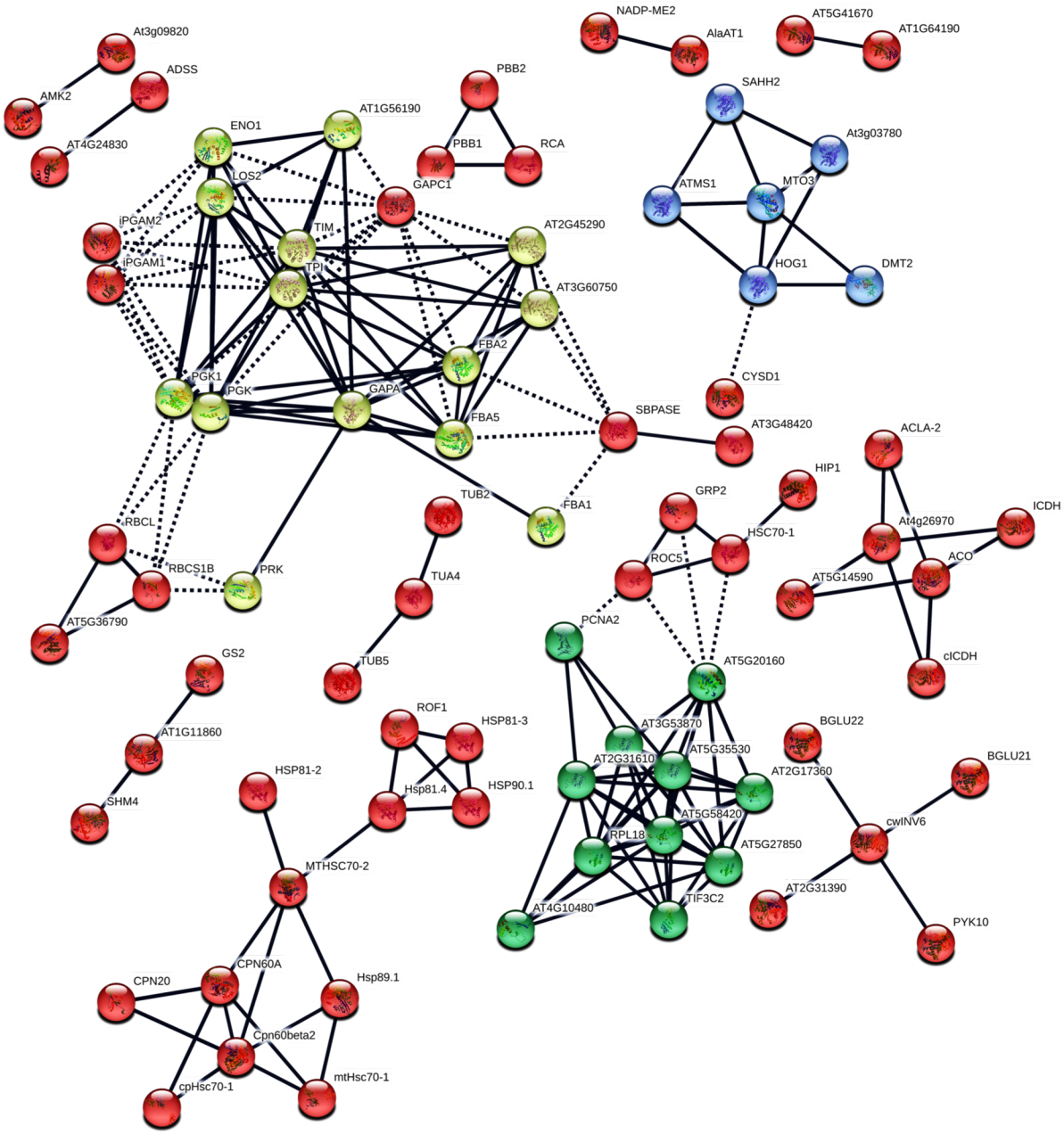

Figure 3. Protein-protein interaction network of identified S-cyanylated proteins in leaf and root tissues. Round nodes represents proteins, and lines edges represent interactions. Dashed lines represent inter-cluster edges. Node modules indicated in red, yellow, blue and green colors were identified by *k*-means clustering.

A

Sedoheptulose 1, 7-bisphosphatase
Protein sequence coverage: 67%
Peptide score: 123

```
METSIACYSR GILPPSVSSQ RSSTLVSPPS YSTSSSFKRL KSSSIFGDSL 50
RLAPKSQLKA TKAKSNGAST VTKCEIGQSL EEFLAQATPD KGLRTLLMCM 100
GEALRTIAFK VRTASCGGTA CVNSFGDEQL AVDMLADKLL FEALQYSHVC 150
KYACSEEVPE LQDMGGPVEG GFSVAFDPLD GSSIVDTNFT VGTIFGVWPG 200
DKLTGITGGD QVAAAMGIYG PRTTYVLAVK GFPGTHEFLL LDEGKWQHVK 250
ETTEIAEGKM FSPGNLRATF DNSEYSKLID YYVKEKYTLR YTGGMVPDVN 300
QIIVKEKGIF TNVTSPTAKA KLRLLFEVAP LGLLIENAGG FSSDGHKSVL 350
DKTIINLDDR TQVAYGSKNE IIRFEETLYG TSRLKNVPIG VTA 393
```

^{64}SNGASTVTKC$_{[CN]}$EIGQSLEEFLAQATPDK^{90}

y$_{13}$ y$_{11}$ y$_{10}$ y$_{9}$

b$_{10}$

B

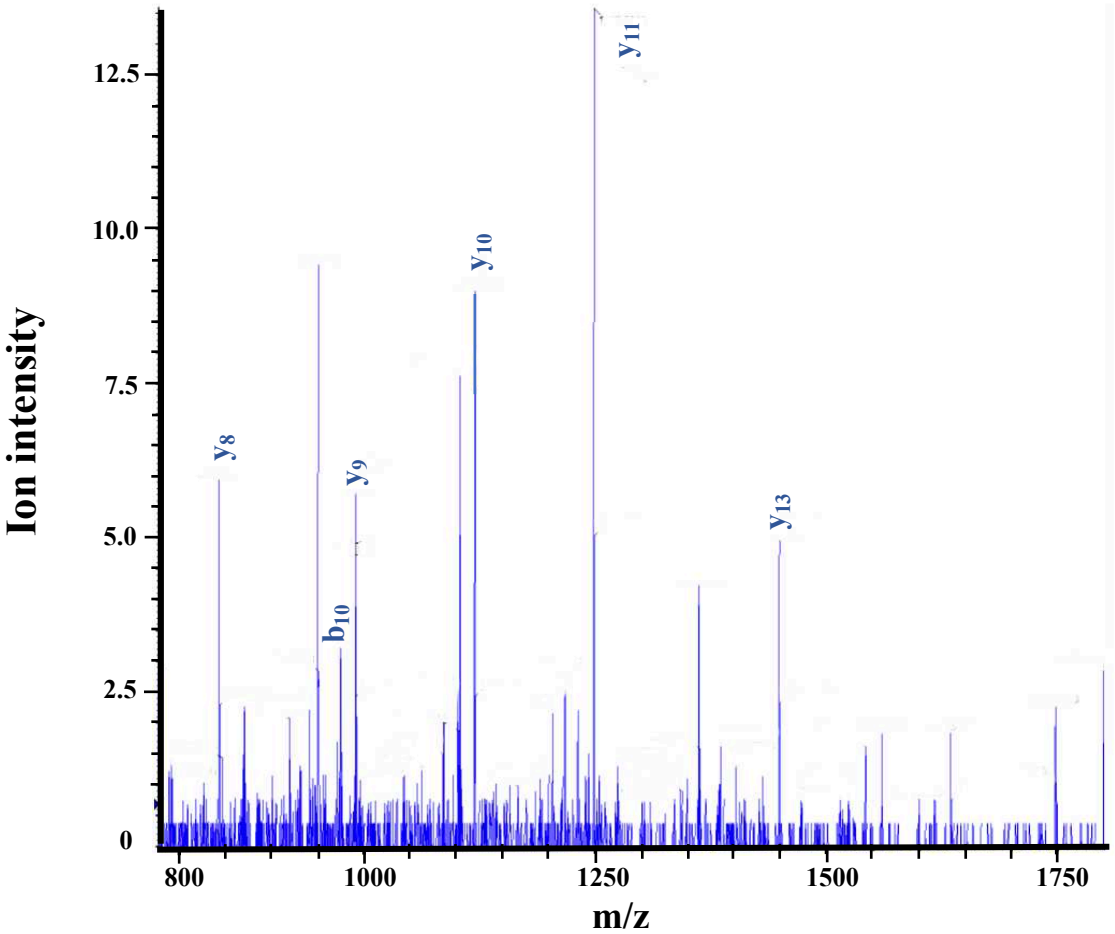

Figure 4. Identification of sedoheptulose 1, 7-bisphosphatase using mass spectrometry. (A) The protein was identified with a sequence coverage of 67%. The identified peptides are shown in red and the peptide containing S-cyanylated Cys^{74} is underlined. The modified Cys residue is shown in blue color. (B) Mass spectrum from the LC-MS/MS analysis of the tryptic peptide containing Cys^{74} of SBPase . Predicted ion types and the detected ions are shown in Table S11.

A

Peptidyl-prolyl cis-trans isomerase CYP20-3
Protein sequence coverage: 61%
Peptide score: 75.6

```
MASSSSMQMV HTSRSIAQIG FGVKSQLVSA NRTTQSVCFG ARSSGIALSS 50
RLHYASPIKQ FSGVYATTKH QRTACVKSMA AEEEEVIEPQ AKVTNKVYFD 100
VEIGGEVAGR IVMGLFGEVV PKTVENFRAL CTGEKKYGYK GSSFHRIIKD 150
FMIQGGDFTE GNGTGGISIY GAKFEDENFT LKHTGPGILS MANAGPNTNG 200
SQFFICTVKT SWLDNKHVVF GQVIEGMKLV RTLESQETRA FDVPKKGCRI 250
YACGELPLDA 260
```

^{181}H T G P G I L S M A N A G P N T N G S Q F F I C$_{[CN]}$ T V K^{209}

b$_2$ b$_5$ b$_6$ b$_7$ b$_8$ b$_9$ b$_{10}$ b$_{12}$ b$_{13}$ b$_{15}$ b$_{16}$ y$_{15}$ y$_{11}$ y$_9$ y$_7$ y$_4$ y$_3$

B

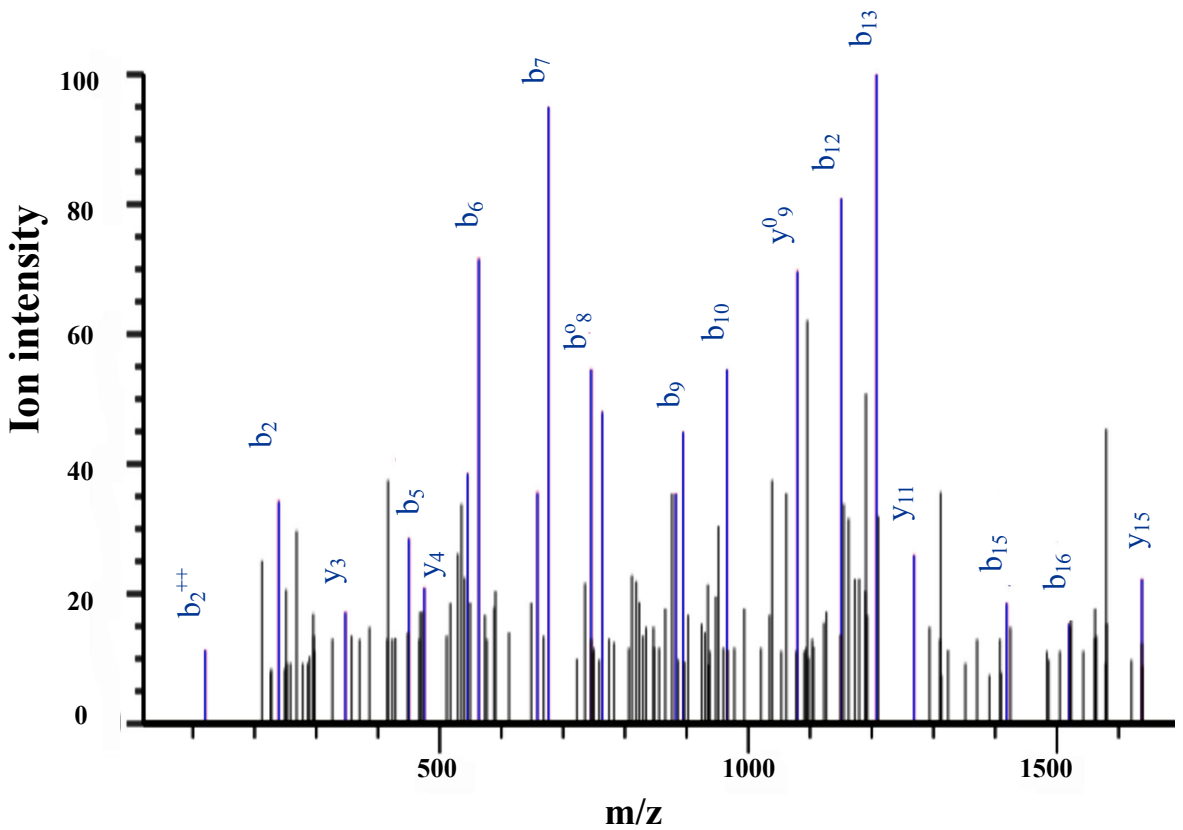

Figure 5. Identification of peptidyl-prolyl cis-trans isomerase CYP20-3 using mass spectrometry. (A) The protein was identified with a sequence coverage of 61%. The identified peptides are shown in red, and the peptide containing S-cyanylated Cys^{206} is underlined. The modified Cys residue is shown in blue color. (B) Mass spectrum from the LC-MS/MS analysis of the tryptic peptide containing Cys^{206} of CYP20-3. Predicted ion types and the detected ions are shown in Table S12.

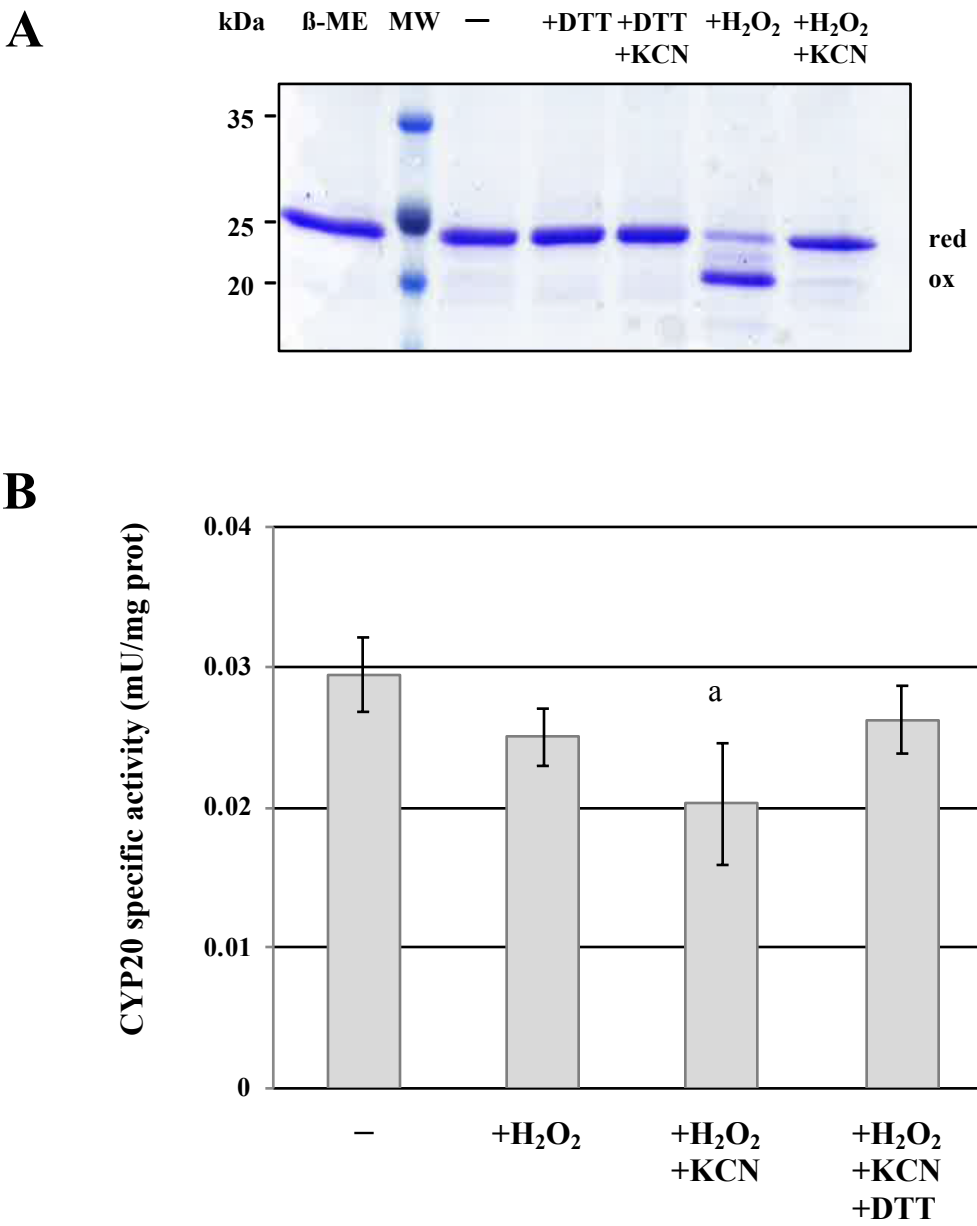

Figure 6. Protein mobility shift and enzymatic activity assays of CYP20-3. (A) Alkylation of purified CYP20-3 protein without any treatment (-); after a 20 min treatment with 0.1 mM DTT (+DTT); after a sequential treatment of 20 min with 0.1 mM DTT and 20 additional min with 1 mM KCN (+DTT+KCN); after a treatment of 20 min 0.1 mM H_2O_2 (+H_2O_2); or after a sequential treatment of 20 min 0.1 mM H_2O_2 and additional 20 min with 1 mM KCN (+H_2O_2+KCN). The first lane (+ß-ME) corresponds to the non-alkylated, ß-mercaptoethanol-reduced protein. MW, molecular weight markers. Reduced (red) and oxidized (ox) forms are indicated. (B) Enzymatic activity of purified CYP20-3 protein without any treatment (-); after a 20 min treatment with 0.1 mM H_2O_2 (+H_2O_2); after a sequential treatment of 20 min with 0.1 mM H_2O_2 and 20 additional min with 1 mM KCN (+H_2O_2+KCN); or after a sequential treatment of 20 min with 0.1 mM H_2O_2, 20 additional min with 1 mM KCN (+H_2O_2+KCN) and 20 additional min with 10 mM DTT (+H_2O_2+KCN+DTT). All results are shown as the mean ± SD (n = 3). a, Significant differences with control sample ($P < 0.05$, one-way ANOVA).

A

Enolase 2, ENO2
Protein sequence coverage: 64%
Peptide score: 75.6

```
MATITVVKAR QIFDSRGNPT VEVDIHTSNG IKVTAAVPSG ASTGIYEALE 50
LRDGGSDYLG KGVSKAVGNV NNIIGPALIG KDPTQQTAID NFMVHELDGT 100
QNEWGWCKQK LGANAILAVS LAVCKAGAVV SGIPLYKHIA NLAGNPKIVL 150
PVPAFNVING GSHAGNKLAM QEFMILPVGA ASFKEAMKMG VEVYHHLKSV 200
IKKKYGQDAT NVGDEGGFAP NIQENKEGLE LLKTAIEKAG YTGKVVIGMD 250
VAASEFYSED KTYDLNFKEE NNNGSQKISG DALKDLYKSF VAEYPIVSIE 300
DPFDQDDWEH YAKMTTECGT EVQIVGDDLL VTNPKRVAKA IAEKSCNALL 350
LKVNQIGSVT ESIEAVKMSK KAGWGVMTSH RSGETEDTFI ADLAVGLSTG 400
QIKTGAPCRS ERLAKYNQLL RIEEELGSEA IYAGVNFRKP VEPY 444
```

^{345}SC$_{[CN]}$NALLLK^{351}

y$_6$ y$_5$ y$_3$ y$_2$ y$_1$

b$_2$ b$_3$ b$_4$ b$_5$ b$_6$ b$_7$

B

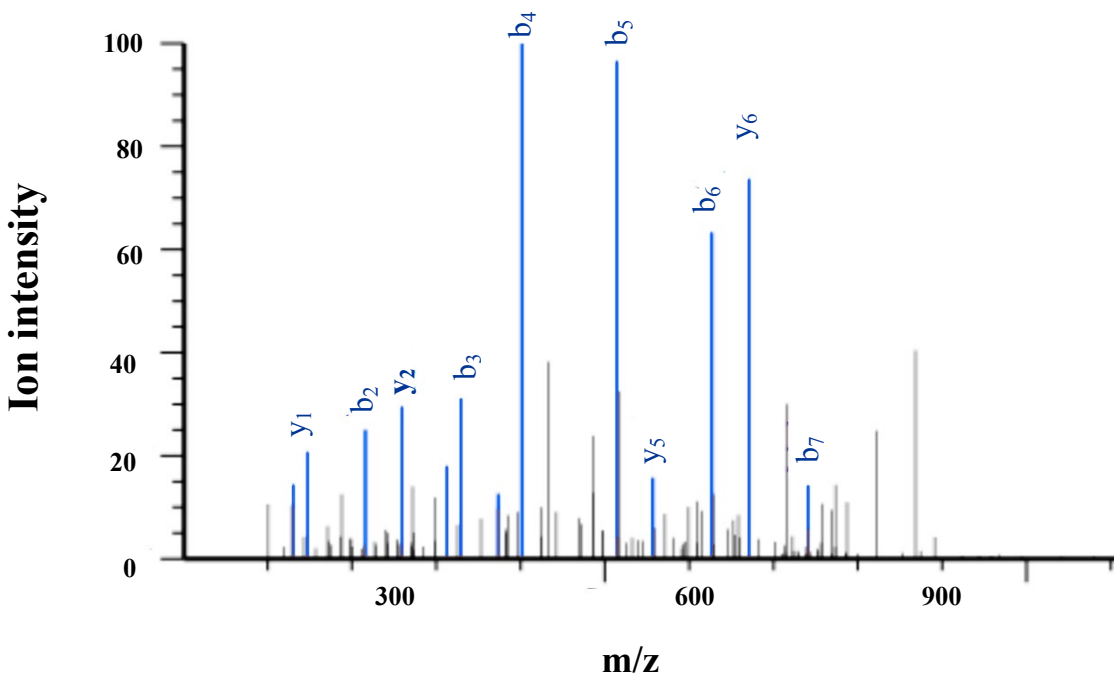

Figure 7. Identification of enolase ENO2 using mass spectrometry. (A) The protein was identified with a sequence coverage of 64%. The peptides identified are shown in red, and the peptide containing S-cyanylated Cys^{346} is underlined. The modified Cys residue is shown in blue color. (B) Mass spectrum from LC-MS/MS analysis of the tryptic peptide containing the Cys^{346} of ENO2. Predicted ion types and the detected ions are shown in Table S13.

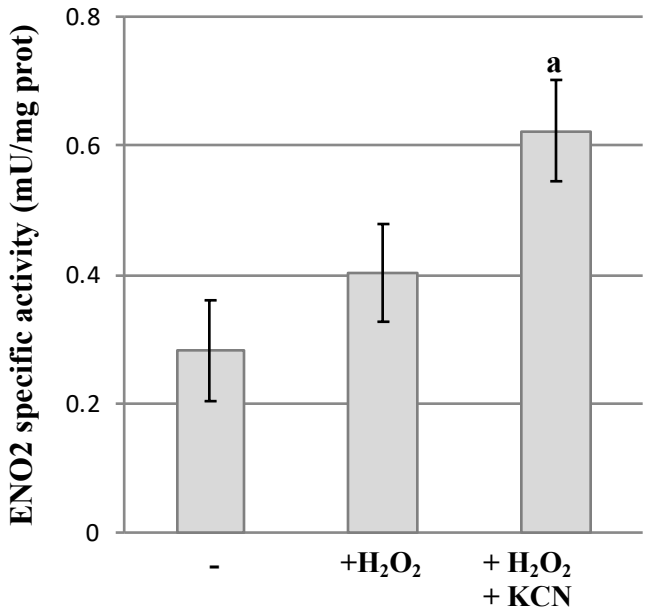

Figure 8. Enzymatic assay of ENO2. Enolase activity of purified ENO2 protein without any treatment (-), after a 20 min treatment with 0.1 mM H_2O_2 (+H_2O_2), or after a sequential treatment of 20 min with 0.1 mM H_2O_2 and 20 additional min with 1 mM KCN (+H_2O_2+KCN). All results are shown as the mean ± SD (n = 6). a, Significant differences with control sample ($P < 0.05$, one-way ANOVA).

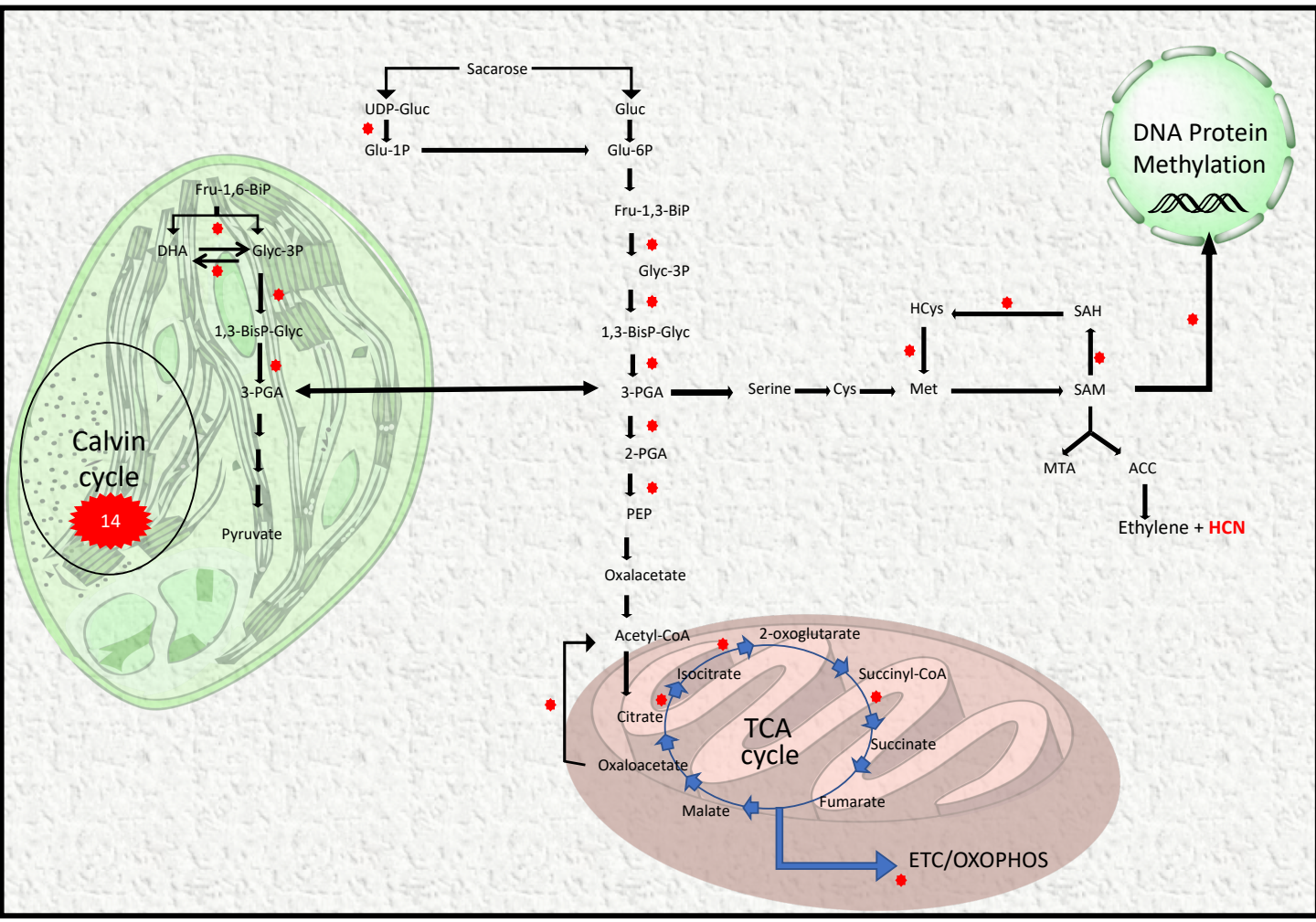

Figure 9. Schematic representation of significant metabolic pathways regulated by S-cyanylation. Red stars mark proteins that can be posttranslationally modified by hydrogen cyanide. The number inside the red star at the Calvin cycle represents the number of proteins. TCA, tricarboxylic acid cycle; ETC/OXOPHOS, electron transport chain and oxidative phosphorylation; SAM, S-adenosyl methionine; SAH, S-adenosyl homocysteine

Parsed Citations

Alvarez, C., García, I., Romero, L.C., Gotor, C. (2012). Mitochondrial Sulfide Detoxification Requires a Functional Isoform O-Acetylserine(thiol)lyase C in Arabidopsis thaliana. Mol Plant 5: 1217-1226.
Pubmed: Author and Title
Google Scholar: Author Only Title Only Author and Title

Alvarez, C., Lozano-Juste, J., Romero, L.C., Garcia, I., Gotor, C., Leon, J. (2011). Inhibition of Arabidopsis O-acetylserine(thiol)lyase A1 by tyrosine nitration. J Biol Chem 286: 578-586.
Pubmed: Author and Title
Google Scholar: Author Only Title Only Author and Title

Anderson, L.E., Li, A.D., Stevens, F.J. (1998). The enolases of ice plant and Arabidopsis contain a potential disulphide and are redox sensitive. Phytochemistry 47: 707-713.
Pubmed: Author and Title
Google Scholar: Author Only Title Only Author and Title

Arenas-Alfonseca, L., Gotor, C., Romero, L.C., Garcia, I. (2018). ß-Cyanoalanine Synthase Action in Root Hair Elongation is Exerted at Early Steps of the Root Hair Elongation Pathway and is Independent of Direct Cyanide Inactivation of NADPH Oxidase. Plant Cell Physiol 59: 1072-1083.
Pubmed: Author and Title
Google Scholar: Author Only Title Only Author and Title

Aroca, A., Gotor, C., Romero, L.C. (2018). Hydrogen Sulfide Signaling in Plants: Emerging Roles of Protein Persulfidation. Front Plant Sci 9.
Pubmed: Author and Title
Google Scholar: Author Only Title Only Author and Title

Aroca, A., Benito, J.M., Gotor, C., Romero, L.C. (2017a). Persulfidation proteome reveals the regulation of protein function by hydrogen sulfide in diverse biological processes in Arabidopsis. J Exp Bot 68: 4915-4927.
Pubmed: Author and Title
Google Scholar: Author Only Title Only Author and Title

Aroca, A., Schneider, M., Scheibe, R., Gotor, C., Romero, L.C. (2017b). Hydrogen Sulfide Regulates the Cytosolic/Nuclear Partitioning of Glyceraldehyde-3-Phosphate Dehydrogenase by Enhancing its Nuclear Localization. Plant Cell Physiol 58: 983-992.
Pubmed: Author and Title
Google Scholar: Author Only Title Only Author and Title

Aroca, Á., Serna, A., Gotor, C., Romero, L.C. (2015). S-Sulfhydration: A Cysteine Posttranslational Modification in Plant Systems. Plant Physiol 168: 334-342.
Pubmed: Author and Title
Google Scholar: Author Only Title Only Author and Title

Baskar, V., Park, S.W., Nile, S.H. (2016). An Update on Potential Perspectives of Glucosinolates on Protection against Microbial Pathogens and Endocrine Dysfunctions in Humans. Crit Rev Food Sci Nutr 56: 2231-2249.
Pubmed: Author and Title
Google Scholar: Author Only Title Only Author and Title

Berg, S.P., Krogmann, D.W. (1975). Mechanism of KCN inhibition of photosystem I. J Biol Chem 250: 8957-8962.
Pubmed: Author and Title
Google Scholar: Author Only Title Only Author and Title

Bermudez, M.A., Paez-Ochoa, M.A., Gotor, C., Romero, L.C. (2010). Arabidopsis S-sulfocysteine synthase activity is essential for chloroplast function and long-day light-dependent redox control. Plant Cell 22: 403-416.
Pubmed: Author and Title
Google Scholar: Author Only Title Only Author and Title

Bermudez, M.A., Galmes, J., Moreno, I., Mullineaux, P.M., Gotor, C., Romero, L.C. (2012). Photosynthetic adaptation to length of day is dependent on S-sulfocysteine synthase activity in the thylakoid lumen. Plant Physiol 160: 274-288.
Pubmed: Author and Title
Google Scholar: Author Only Title Only Author and Title

Bethke, P.C., Libourel, L.G.L., Reinohl, V., Jones, R.L. (2006). Sodium nitroprusside, cyanide, nitrite, and nitrate break Arabidopsis seed dormancy in a nitric oxide-dependent manner. Planta 223: 805-812.
Pubmed: Author and Title
Google Scholar: Author Only Title Only Author and Title

Bishop, N.I., Spikes, J.D. (1955). Inhibition by Cyanide of the Photochemical Activity of Isolated Chloroplasts. Nature 176: 307-308.
Pubmed: Author and Title
Google Scholar: Author Only Title Only Author and Title

Bottcher, C., Westphal, L., Schmotz, C., Prade, E., Scheel, D., Glawischnig, E. (2009). The multifunctional enzyme CYP71B15 (PHYTOALEXIN DEFICIENT3) converts cysteine-indole-3-acetonitrile to camalexin in the indole-3-acetonitrile metabolic network of Arabidopsis thaliana. Plant Cell 21: 1830-1845.

Pubmed: Author and Title
Google Scholar: Author Only Title Only Author and Title

Boukouris, A.E., Zervopoulos, S.D., Michelakis, E.D. (2016). Metabolic Enzymes Moonlighting in the Nucleus: Metabolic Regulation of Gene Transcription. Trends Biochem Sci 41: 712-730.
Pubmed: Author and Title
Google Scholar: Author Only Title Only Author and Title

Buchanan, B.B., Balmer, Y. (2005). Redox regulation: a broadening horizon. Annu Rev Plant Biol 56: 187-220.
Pubmed: Author and Title
Google Scholar: Author Only Title Only Author and Title

Catsimpoolas, N., Wood, J.L. (1966). Specific cleavage of cystine peptides by cyanide. J Biol Chem 241: 1790-1796.
Pubmed: Author and Title
Google Scholar: Author Only Title Only Author and Title

Chen, Z. (2001). A superfamily of proteins with novel cysteine-rich repeats. Plant Physiol 126: 473-476.
Pubmed: Author and Title
Google Scholar: Author Only Title Only Author and Title

Chivasa, S., Carr, J.P. (1998). Cyanide restores N gene-mediated resistance to tobacco mosaic virus in transgenic tobacco expressing salicylic acid hydroxylase. Plant Cell 10: 1489-1498.
Pubmed: Author and Title
Google Scholar: Author Only Title Only Author and Title

Cohen, W.S., McCarty, R.E. (1976). Reversibility of the cyanide inhibition of electron transport in spinach chloroplast thylakoids. Biochem Biophys Res Commun 73: 679-685.
Pubmed: Author and Title
Google Scholar: Author Only Title Only Author and Title

Eremina, M., Rozhon, W., Yang, S., Poppenberger, B. (2015). ENO2 activity is required for the development and reproductive success of plants, and is feedback-repressed by AtMBP-1. Plant J 81: 895-906.
Pubmed: Author and Title
Google Scholar: Author Only Title Only Author and Title

Fasco, M.J., Iii, C.R., Stack, R.F., O'Hehir, C., Barr, J.R., Eadon, G.A. (2007). Cyanide adducts with human plasma proteins: albumin as a potential exposure surrogate. Chem Res Toxicol 20: 677-684.
Pubmed: Author and Title
Google Scholar: Author Only Title Only Author and Title

Fricker, L.D. (2015). Limitations of Mass Spectrometry-Based Peptidomic Approaches. J Am Soc Mass Spectrom 26: 1981-1991.
Pubmed: Author and Title
Google Scholar: Author Only Title Only Author and Title

Fukano, K., Kimura, K. (2014). Measurement of enolase activity in cell lysates. Methods Enzymol 542: 115-124.
Pubmed: Author and Title
Google Scholar: Author Only Title Only Author and Title

Garcia, I., Gotor, C., Romero, L.C. (2014). Beyond toxicity: A regulatory role for mitochondrial cyanide. Plant Signal Behav 9: e27612.
Pubmed: Author and Title
Google Scholar: Author Only Title Only Author and Title

Garcia, I., Rosas, T., Bejarano, E.R., Gotor, C., Romero, L.C. (2013). Transient transcriptional regulation of the CYS-C1 gene and cyanide accumulation upon pathogen infection in the plant immune response. Plant Physiol 162: 2015-2027.
Pubmed: Author and Title
Google Scholar: Author Only Title Only Author and Title

Garcia, I., Castellano, J.M., Vioque, B., Solano, R., Gotor, C., Romero, L.C. (2010). Mitochondrial beta-cyanoalanine synthase is essential for root hair formation in Arabidopsis thaliana. Plant Cell 22: 3268-3279.
Pubmed: Author and Title
Google Scholar: Author Only Title Only Author and Title

Gawron, O. (1966). CHAPTER 14 - ON THE REACTION OF CYANIDE WITH CYSTINE AND CYSTINE PEPTIDES. In The Chemistry of Organic Sulfur Compounds (Pergamon), pp. 351-365.
Pubmed: Author and Title
Google Scholar: Author Only Title Only Author and Title

Geigenberger, P., Kolbe, A., Tiessen, A. (2005). Redox regulation of carbon storage and partitioning in response to light and sugars. J Exp Bot 56: 1469-1479.
Pubmed: Author and Title
Google Scholar: Author Only Title Only Author and Title

Giege, P., Heazlewood, J.L., Roessner-Tunali, U., Millar, A.H., Fernie, A.R., Leaver, C.J., Sweetlove, L.J. (2003). Enzymes of glycolysis are functionally associated with the mitochondrion in Arabidopsis cells. Plant Cell 15: 2140-2151.
Pubmed: Author and Title

Google Scholar: Author Only Title Only Author and Title

Gotor, C., Laureano-Marín, A.M., Arenas-Alfonseca, L., Moreno, I., Aroca, Á., García, I., Romero, L.C. (2017). Advances in Plant Sulfur Metabolism and Signaling. In Progress in Botany Vol. 78, F M Cánovas, U Lüttge,R Matyssek, eds (Cham: Springer International Publishing), pp. 45-66.
Pubmed: Author and Title
Google Scholar: Author Only Title Only Author and Title

Grierson, C., Nielsen, E., Ketelaarc, T., Schiefelbein, J. (2014). Root hairs. Arabidopsis Book 12: e0172.
Pubmed: Author and Title
Google Scholar: Author Only Title Only Author and Title

Grigoryan, H., Edmands, W., Lu, S.S., Yano, Y., Regazzoni, L., Iavarone, A.T., Williams, E.R., Rappaport, S.M. (2016). Adductomics Pipeline for Untargeted Analysis of Modifications to Cys34 of Human Serum Albumin. Anal Chem 88: 10504-10512.
Pubmed: Author and Title
Google Scholar: Author Only Title Only Author and Title

Hanschen, F.S., Lamy, E., Schreiner, M., Rohn, S. (2014). Reactivity and stability of glucosinolates and their breakdown products in foods. Angew Chem Int Ed Engl 53: 11430-11450.
Pubmed: Author and Title
Google Scholar: Author Only Title Only Author and Title

Harmel, R., Fiedler, D. (2018). Features and regulation of non-enzymatic post-translational modifications. Nat Chem Biol 14: 244.
Pubmed: Author and Title
Google Scholar: Author Only Title Only Author and Title

Hatzfeld, Y., Maruyama, A., Schmidt, A., Noji, M., Ishizawa, K., Saito, K. (2000). beta-Cyanoalanine synthase is a mitochondrial cysteine synthase-like protein in spinach and Arabidopsis. Plant Physiol 123: 1163-1171.
Pubmed: Author and Title
Google Scholar: Author Only Title Only Author and Title

Holtgrefe, S., Gohlke, J., Starmann, J., Druce, S., Klocke, S., Altmann, B., Wojtera, J., Lindermayr, C., Scheibe, R. (2008). Regulation of plant cytosolic glyceraldehyde 3-phosphate dehydrogenase isoforms by thiol modifications. Physiol Plant 133: 211-228.
Pubmed: Author and Title
Google Scholar: Author Only Title Only Author and Title

Isom, G.E., Way, J.L. (1984). Effects of oxygen on the antagonism of cyanide intoxication: cytochrome oxidase, in vitro. Toxicol Appl Pharmacol 74: 57-62.
Pubmed: Author and Title
Google Scholar: Author Only Title Only Author and Title

Jacobson, G.R., Schaffer, M.H., Stark, G.R., Vanaman, T.C. (1973). Specific chemical cleavage in high yield at the amino peptide bonds of cysteine and cystine residues. J Biol Chem 248: 6583-6591.
Pubmed: Author and Title
Google Scholar: Author Only Title Only Author and Title

Jeong, J.S., Jung, C., Seo, J.S., Kim, J.K., Chua, N.H. (2017). The Deubiquitinating Enzymes UBP12 and UBP13 Positively Regulate MYC2 Levels in Jasmonate Responses. Plant Cell 29: 1406-1424.
Pubmed: Author and Title
Google Scholar: Author Only Title Only Author and Title

Klie, S., Nikoloski, Z. (2012). The Choice between MapMan and Gene Ontology for Automated Gene Function Prediction in Plant Science. Front Genet 3: 115.
Pubmed: Author and Title
Google Scholar: Author Only Title Only Author and Title

Knowles, C.J. (1976). Microorganisms and cyanide. Bacteriol Rev 40: 652-680.
Pubmed: Author and Title
Google Scholar: Author Only Title Only Author and Title

Laemmli, U.K. (1970). Cleavage of structural proteins during the assembly of the head of bacteriophage T4. Nature 227: 680-685.
Pubmed: Author and Title
Google Scholar: Author Only Title Only Author and Title

Lee, H., Guo, Y., Ohta, M., Xiong, L., Stevenson, B., Zhu, J.K. (2002). LOS2, a genetic locus required for cold-responsive gene transcription encodes a bi-functional enolase. EMBO J 21: 2692-2702.
Pubmed: Author and Title
Google Scholar: Author Only Title Only Author and Title

Lee, S., Doxey, A.C., McConkey, B.J., Moffatt, B.A. (2012). Nuclear targeting of methyl-recycling enzymes in Arabidopsis thaliana is mediated by specific protein interactions. Mol Plant 5: 231-248.
Pubmed: Author and Title
Google Scholar: Author Only Title Only Author and Title

Lozano-Durán, R., García, I., Huguet, S., Balzergue, S., Romero, L.C., Bejarano, E.R. (2012). Geminivirus C2 protein represses genes

involved in sulphur assimilation and this effect can be counteracted by jasmonate treatment. Eur J Plant Pathol 134: 49-59.
Pubmed: Author and Title
Google Scholar: Author Only Title Only Author and Title

Mi, H., Huang, X., Muruganujan, A., Tang, H., Mills, C., Kang, D., Thomas, P.D. (2017). PANTHER version 11: expanded annotation data from Gene Ontology and Reactome pathways, and data analysis tool enhancements. Nucleic Acids Res 45: D183-d189.
Pubmed: Author and Title
Google Scholar: Author Only Title Only Author and Title

Moller, I.M., Rogowska-Wrzesinska, A., Rao, R.S. (2011). Protein carbonylation and metal-catalyzed protein oxidation in a cellular perspective. J Proteomics 74: 2228-2242.
Pubmed: Author and Title
Google Scholar: Author Only Title Only Author and Title

Monaghan, J., Xu, F., Gao, M., Zhao, Q., Palma, K., Long, C., Chen, S., Zhang, Y., Li, X. (2009). Two Prp19-like U-box proteins in the MOS4-associated complex play redundant roles in plant innate immunity. PLoS Pathog 5: e1000526.
Pubmed: Author and Title
Google Scholar: Author Only Title Only Author and Title

Motohashi, K., Koyama, F., Nakanishi, Y., Ueoka-Nakanishi, H., Hisabori, T. (2003). Chloroplast cyclophilin is a target protein of thioredoxin. Thiol modulation of the peptidyl-prolyl cis-trans isomerase activity. J Biol Chem 278: 31848-31852.
Pubmed: Author and Title
Google Scholar: Author Only Title Only Author and Title

Nguema-Ona, E., Bannigan, A., Chevalier, L., Baskin, T.I., Driouich, A. (2007). Disruption of arabinogalactan proteins disorganizes cortical microtubules in the root of Arabidopsis thaliana. Plant J 52: 240-251.
Pubmed: Author and Title
Google Scholar: Author Only Title Only Author and Title

Nicholls, P., Marshall, D.C., Cooper, C.E., Wilson, M.T. (2013). Sulfide inhibition of and metabolism by cytochrome c oxidase. Biochem Soc Trans 41: 1312-1316.
Pubmed: Author and Title
Google Scholar: Author Only Title Only Author and Title

Ortea, I., Ruiz-Sanchez, I., Canete, R., Caballero-Villarraso, J., Canete, M.D. (2018). Identification of candidate serum biomarkers of childhood-onset growth hormone deficiency using SWATH-MS and feature selection. J Proteomics 175: 105-113.
Pubmed: Author and Title
Google Scholar: Author Only Title Only Author and Title

Park, C.-M., Weerasinghe, L., Day, J.J., Fukuto, J.M., Xian, M. (2015). Persulfides: Current Knowledge and Challenges in Chemistry and Chemical Biology. Molecular bioSystems 11: 1775-1785.
Pubmed: Author and Title
Google Scholar: Author Only Title Only Author and Title

Peiser, G.D., Wang, T.T., Hoffman, N.E., Yang, S.F., Liu, H.W., Walsh, C.T. (1984). Formation of cyanide from carbon 1 of 1-aminocyclopropane-1-carboxylic acid during its conversion to ethylene. Proc Natl Acad Sci U S A 81: 3059-3063.
Pubmed: Author and Title
Google Scholar: Author Only Title Only Author and Title

Rao, R.S.P., Salvato, F., Thal, B., Eubel, H., Thelen, J.J., Møller, I.M. (2017). The proteome of higher plant mitochondria. Mitochondrion 33: 22-37.
Pubmed: Author and Title
Google Scholar: Author Only Title Only Author and Title

Ressler, C., Giza, Y.H., Nigam, S.N. (1969). ß-Cyanoalanine, product of cyanide fixation and intermediate in asparagine biosynthesis in certain species of Lathyrus and Vicia. J Am Chem Soc 91: 2766-2775.
Pubmed: Author and Title
Google Scholar: Author Only Title Only Author and Title

Rocha, P.S., Sheikh, M., Melchiorre, R., Fagard, M., Boutet, S., Loach, R., Moffatt, B., Wagner, C., Vaucheret, H., Furner, I. (2005). The Arabidopsis HOMOLOGY-DEPENDENT GENE SILENCING1 gene codes for an S-adenosyl-L-homocysteine hydrolase required for DNA methylation-dependent gene silencing. Plant Cell 17: 404-417.
Pubmed: Author and Title
Google Scholar: Author Only Title Only Author and Title

Romero, L.C., Aroca, M.A., Laureano-Marin, A.M., Moreno, I., Garcia, I., Gotor, C. (2014). Cysteine and cysteine-related signaling pathways in Arabidopsis thaliana. Mol Plant 7: 264-276.
Pubmed: Author and Title
Google Scholar: Author Only Title Only Author and Title

Salvato, F., Havelund, J.F., Chen, M., Rao, R.S.P., Rogowska-Wrzesinska, A., Jensen, O.N., Gang, D.R., Thelen, J.J., Møller, I.M. (2014). The Potato Tuber Mitochondrial Proteome. Plant Physiol 164: 637-653.
Pubmed: Author and Title
Google Scholar: Author Only Title Only Author and Title

Sauter, M., Moffatt, B., Saechao, M.C., Hell, R., Wirtz, M. (2013). Methionine salvage and S-adenosylmethionine: essential links between sulfur, ethylene and polyamine biosynthesis. Biochem J 451: 145-154.
Pubmed: Author and Title
Google Scholar: Author Only Title Only Author and Title

Seo, S., Mitsuhara, I., Feng, J., Iwai, T., Hasegawa, M., Ohashi, Y. (2011). Cyanide, a coproduct of plant hormone ethylene biosynthesis, contributes to the resistance of rice to blast fungus. Plant Physiol 155: 502-514.
Pubmed: Author and Title
Google Scholar: Author Only Title Only Author and Title

Struglics, A., Fredlund, K.M., Rasmusson, A.G., Møller, I.M. (1993). The presence of a short redox chain in the membrane of intact potato tuber peroxisomes and the association of malate dehydrogenase with the peroxisomal membrane. Physiol Plant 88: 19-28.
Pubmed: Author and Title
Google Scholar: Author Only Title Only Author and Title

Szklarczyk, D., Morris, J.H., Cook, H., Kuhn, M., Wyder, S., Simonovic, M., Santos, A., Doncheva, N.T., Roth, A., Bork, P., Jensen, L.J., von Mering, C. (2017). The STRING database in 2017: quality-controlled protein-protein association networks, made broadly accessible. Nucleic Acids Res 45: D362-d368.
Pubmed: Author and Title
Google Scholar: Author Only Title Only Author and Title

Szklarczyk, D., Franceschini, A., Wyder, S., Forslund, K., Heller, D., Huerta-Cepas, J., Simonovic, M., Roth, A., Santos, A., Tsafou, K.P., Kuhn, M., Bork, P., Jensen, L.J., von Mering, C. (2015). STRING v10: protein-protein interaction networks, integrated over the tree of life. Nucleic Acids Res 43: D447-452.
Pubmed: Author and Title
Google Scholar: Author Only Title Only Author and Title

Tang, D., Wang, G., Zhou, J.-M. (2017). Receptor Kinases in Plant-Pathogen Interactions: More Than Pattern Recognition. The Plant Cell 29: 618-637.
Pubmed: Author and Title
Google Scholar: Author Only Title Only Author and Title

Taylorson, R.B., Hendricks, S.B. (1973). Promotion of seed germination by cyanide. Plant Physiol 52: 23-27.
Pubmed: Author and Title
Google Scholar: Author Only Title Only Author and Title

Thimm, O., Blasing, O., Gibon, Y., Nagel, A., Meyer, S., Kruger, P., Selbig, J., Muller, L.A., Rhee, S.Y., Stitt, M. (2004). MAPMAN: a user-driven tool to display genomics data sets onto diagrams of metabolic pathways and other biological processes. Plant J 37: 914-939.
Pubmed: Author and Title
Google Scholar: Author Only Title Only Author and Title

Thompson, J.P., Marrs, T.C. (2012). Hydroxocobalamin in cyanide poisoning. Clinical toxicology (Philadelphia, Pa 50: 875-885.
Pubmed: Author and Title
Google Scholar: Author Only Title Only Author and Title

Tinajero-Trejo, M., Jesse, H.E., Poole, R.K. (2013). Gasotransmitters, poisons, and antimicrobials: it's a gas, gas, gas! F1000Prime Rep 5: 28.
Pubmed: Author and Title
Google Scholar: Author Only Title Only Author and Title

Trebst, A.V., Losada, M., Arnon, D.I. (1960). Photosynthesis by isolated chloroplasts. XII. Inhibitors of carbon dioxide assimilation in a reconstituted chloroplast system. J Biol Chem 235: 840-844.
Pubmed: Author and Title
Google Scholar: Author Only Title Only Author and Title

Vizcaino, J.A., Csordas, A., del-Toro, N., Dianes, J.A., Griss, J., Lavidas, I., Mayer, G., Perez-Riverol, Y., Reisinger, F., Ternent, T., Xu, Q.W., Wang, R., Hermjakob, H. (2016). 2016 update of the PRIDE database and its related tools. Nucleic Acids Res 44: D447-456.
Pubmed: Author and Title
Google Scholar: Author Only Title Only Author and Title

Vowinckel, J., Capuano, F., Campbell, K., Deery, M.J., Lilley, K.S., Ralser, M. (2013). The beauty of being (label)-free: sample preparation methods for SWATH-MS and next-generation targeted proteomics. F1000Res 2: 272.
Pubmed: Author and Title
Google Scholar: Author Only Title Only Author and Title

Wagner, E.S., Davis, R.E. (1966). Displacement Reactions. IX. The Reaction of Cyanide Ion with Cystine. An Example of Amino Group Participation as Detected with Nitrogen-15 during Cleavage of a Sulfur-Sulfur Bond1. J Am Chem Soc 88: 7-12.
Pubmed: Author and Title
Google Scholar: Author Only Title Only Author and Title

Wang, R. (2014). Gasotransmitters: growing pains and joys. Trends Biochem Sci 39: 227-232.
Pubmed: Author and Title
Google Scholar: Author Only Title Only Author and Title

Williams, S.J., Sohn, K.H., Wan, L., Bernoux, M., Sarris, P.F., Segonzac, C., Ve, T., Ma, Y., Saucet, S.B., Ericsson, D.J., Casey, L.W.,

Lonhienne, T., Winzor, D.J., Zhang, X., Coerdt, A., Parker, J.E., Dodds, P.N., Kobe, B., Jones, J.D. (2014). Structural basis for assembly and function of a heterodimeric plant immune receptor. Science 344: 299-303.
Pubmed: Author and Title
Google Scholar: Author Only Title Only Author and Title

Wong, C.E., Carson, R.A., Carr, J.P. (2002). Chemically induced virus resistance in Arabidopsis thaliana is independent of pathogenesis-related protein expression and the NPR1 gene. Mol Plant Microbe Interact 15: 75-81.
Pubmed: Author and Title
Google Scholar: Author Only Title Only Author and Title

Wu, J., Watson, J.T. (1998). Optimization of the cleavage reaction for cyanylated cysteinyl proteins for efficient and simplified mass mapping. Anal Biochem 258: 268-276.
Pubmed: Author and Title
Google Scholar: Author Only Title Only Author and Title

Wu, X., Li, F., Kolenovsky, A., Caplan, A., Cui, Y., Cutler, A., Tsang, E.W.T. (2009). A mutant deficient in S-adenosylhomocysteine hydrolase in Arabidopsis shows defects in root-hair developmentThis paper is one of a selection of papers published in a Special Issue from the National Research Council of Canada – Plant Biotechnology Institute. Botany 87: 571-584.
Pubmed: Author and Title
Google Scholar: Author Only Title Only Author and Title

Yamasaki, H., Watanabe, N.S., Sakihama, Y., Cohen, M.F. (2016). An Overview of Methods in Plant Nitric Oxide (NO) Research: Why Do We Always Need to Use Multiple Methods? Methods Mol Biol 1424: 1-14.
Pubmed: Author and Title
Google Scholar: Author Only Title Only Author and Title

Yip, W.K., Yang, S.F. (1988). Cyanide metabolism in relation to ethylene production in plant tissues. Plant Physiol 88: 473-476.
Pubmed: Author and Title
Google Scholar: Author Only Title Only Author and Title

Zaffagnini, M., Fermani, S., Costa, A., Lemaire, S.D., Trost, P. (2013). Plant cytoplasmic GAPDH: redox post-translational modifications and moonlighting properties. Front Plant Sci 4: 450.
Pubmed: Author and Title
Google Scholar: Author Only Title Only Author and Title

Zhang, D., Macinkovic, I., Devarie-Baez, N.O., Pan, J., Park, C.M., Carroll, K.S., Filipovic, M.R., Xian, M. (2014). Detection of protein S-sulfhydration by a tag-switch technique. Angew Chem Int Ed Engl 53: 575-581.
Pubmed: Author and Title
Google Scholar: Author Only Title Only Author and Title

Zidenga, T., Siritunga, D., Sayre, R.T. (2017). Cyanogen Metabolism in Cassava Roots: Impact on Protein Synthesis and Root Development. Front Plant Sci 8: 220.
Pubmed: Author and Title
Google Scholar: Author Only Title Only Author and Title